Table of Contents

Notation

When a function is discussed as a point on the function space, that function is denoted without specifying the independent variables, such as ϕ. By contrast, when we concentrate on the value of the function, this value is denoted with the independent variables, like $\phi(\boldsymbol{x}, E)$. $\boldsymbol{x}$ is a vector describing the position and the direction of neutrons under the transport approximation, and E the energy of neutrons.

When creation operator of neutrons M and annihilation operator L are defined and the system is subcritical, operator Ψ represents the mapping from external neutron source distribution function S to neutron flux distribution function ΨS which satisfies the following equation:

$$L\Psi S = M\Psi S + S \quad . \tag{0.1}$$

In other words, ΨS is the neutron flux distribution function in the steady state with an external neutron source represented by S. When the operators are specified like $\Psi_{M',L'}$, the following equation defines function $\Psi_{M',L'}S$:

$$L'\Psi_{M',L'}S = M'\Psi_{M',L'}S + S \quad . \tag{0.2}$$

The integral of function A over the whole space and energy is represented by $\langle A \rangle$ as follows:

$$\langle A \rangle \equiv \iint A(\boldsymbol{x}, E) \, \mathrm{d}\boldsymbol{x} \, \mathrm{d}E \quad . \tag{0.3}$$

The inner product of real functions A and B is represented by $\langle A, \ B \rangle$, and is defined as

$$\langle A, \ B \rangle \equiv \langle AB \rangle = \iint A(\boldsymbol{x}, E) B(\boldsymbol{x}, E) \, \mathrm{d}\boldsymbol{x} \, \mathrm{d}E \quad . \tag{0.4}$$

§1 Introduction

1.1 Necessity of Subcriticality Measurement and Accelerator Driven Systems

Subcriticality measurement is one of the most important issues for the Accelerator Driven System (ADS) and the fuel reprocessing facility. Subcriticality should be monitored during the operation of ADS, since the reactor power is closely related to the subcriticality. On the other hand, accurate measurement of subcriticality guarantees the criticality safety of nuclear facilities, such as fuel reprocessing facilities. By the rigorous monitoring of subcriticality, the production efficiency of these facilities can be improved without losing the safety. In contrast with this economical importance of the criticality safety, putting ADS to practical use is required in terms of ethics among generations, related to the handling of the radioactive waste.

One of the most significant problems on using nuclear power is handling of the radioactive waste. Although the isotopic composition of the radioactive waste depends on the reactor type, operation period, and so on, some radioactive isotopes with long lifetime are always generated, particularly ^{99}Tc and some actinoids. One of the proposed methods of the treatment of these long-lived radioactive isotopes is to immobilize these isotopes in ceramics, such as glass, and put them in the permanent disposal.[1,2] However, this method includes ethical issues which are similar to those of the problem related with the greenhouse gases.

Since the industrial revolution, human beings have been emitting CO_2 and some other kinds of greenhouse gases. On the other hand, young generations cannot spend much fossil fuel in the future, while they are going to be hit by the desperate calamity of the global warming. In other words, in contrast that old generations were granted only the favour of fossil fuel, young generations obtain only the penalty caused by their ancestors. This inequality is the ethical problem among generations of the greenhouse gases. Similar ethical issues exist in the case of the radioactive waste. Even if the waste is immobilized by ceramics, our guarantee of the safety is quite limited in time. For instance, the location of the permanent disposal might be forgotten by 1,000 years later, and then someone may conduct boring at that place, so that the immobilization would be broken.

Therefore, the lifetime of the monitoring system of the permanent disposal is an important issue. It must be enough longer than the lifetime of the radioactive isotopes. From another viewpoint, the radioactive isotopes which have longer lifetime than the monitoring system should be excluded from the waste. In order to satisfy this condition, transmutation of the long-lived radioactive isotope into a short-lived one is necessary.

Using nuclear reactors is one of the possible methods of the nuclear transmutation.[3] In particular, ADS can play an important role in the strategies of the nuclear transmutation.[4] The advantage of using ADS is that accelerators can generate neutrons with some flexibility in neutron energy spectrum. Irradiated by the neutron beam which has appropriately chosen spectrum for the transmutation, the radioactive waste can be eliminated without producing significant amount of other long-lived radioactive isotopes.[5,6] Therefore, ADS is considered as the most powerful system for the nuclear transmutation.

As a part of the development of ADS, the methods of the subcriticality measurement, which will contribute to the power control of ADS, are discussed in this paper.

1.2 Definition of Subcriticality

Subcriticality $\Delta\rho$ is defined as

$$\Delta\rho \equiv \left| 1 - \frac{1}{k_{\rm eff}} \right| \quad , \tag{1.1}$$

where $k_{\rm eff}$ is called effective multiplication factor. $k_{\rm eff}$ is usually defined as the largest eigenvalue of the system. This definition of $k_{\rm eff}$ is based on the following assumptions: eigenfunctions are assumed to form a complete set; higher modes decrease exponentially faster than the fundamental mode, then they disappear in a short time; therefore only the largest eigenvalue is effective. However, this definition is not theoretically reasonable. As is discussed in Appendix B, the eigenfunctions do not form a complete set. In addition, even if eigenfunctions are assumed to be complete, higher modes remain in the steady subcritical states with external neutron sources. In consequence, the largest eigenvalue is not the only effective eigenvalue.

The following formula is an alternative definition of $k_{\rm eff}$ in the steady subcritical system:

$$k_{\rm eff} \equiv \frac{\langle M\phi_{\rm f}\rangle}{\langle L\phi_{\rm f}\rangle} \quad , \tag{1.2}$$

$$\phi_{\rm f} \equiv \phi - \phi_{\rm s} \quad , \tag{1.3}$$

$$\phi \equiv \Psi S \quad , \tag{1.4}$$

and $\phi_{\rm s}$ is defined as the solution of the following equation:

$$L\phi_{\rm s} = S \quad , \tag{1.5}$$

where M and L are the creation and annihilation operators of neutrons, respectively, and S is the external neutron source distribution function. In this definition, $k_{\rm eff}$ is expressed as the ratio of creation and annihilation of neutrons which are generated by the fission reaction. Neutrons emitted from the external neutron sources are excluded from this ratio. In this paper, ϕ is called *neutron flux distribution function*, ϕ_f *function of neutron flux distribution from fission*, and ϕ_s *function of neutron flux distribution from source*. This $k_{\rm eff}$ is equivalent with fission neutron multiplication rate k_f,[7] which was denoted by k_s in the original paper.[8]

In the steady state, the balance equation of $\phi_{\rm f}$ is

$$L\phi_{\rm f} = M\phi \quad . \tag{1.6}$$

Accordingly, k_{eff} can be calculated by the following equation as well:

$$k_{\mathrm{eff}} = 1 - \frac{\langle M\phi_{\mathrm{s}} \rangle}{\langle M\phi \rangle} \quad . \tag{1.7}$$

When $\langle M\phi_{\mathrm{s}} \rangle$ is approximately constant, reactor power P satisfies

$$P \propto \langle M\phi \rangle \propto \frac{\langle M\phi \rangle}{\langle M\phi_{\mathrm{s}} \rangle} = \frac{1}{1-k} \quad , \tag{1.8}$$

which is strongly related to the subcriticality. Hence, the subcriticality measurement is required for the power control.

1.3 Neutron Source Multiplication Method

In the steady state, the relation between the subcriticality and the count rates of neutron detectors can be theoretically given under some approximations and assumptions. Subcriticality measurement methods based on this relation are called neutron source multiplication method.

1.3.1 Ordinary Neutron Source Multiplication Method

The ordinary neutron source multiplication method is based on the one point reactor approximation. This method is quite simple and inaccurate. The derivation is shown below.

Derivation

The one point reactor approximation is defined as the following approximation:

$$\frac{\phi(\boldsymbol{x},E)}{\varphi_0(\boldsymbol{x},E)} \simeq A \quad , \tag{1.9}$$

where $\phi(\boldsymbol{x},E)$ is the neutron flux distribution function of the system, $\varphi_0(\boldsymbol{x},E)$ the fundamental mode, and A a constant. In the steady subcritical system, Eq. (1.9) can be transformed as follows:

$$\frac{\Psi S(\boldsymbol{x},E)}{\varphi_0(\boldsymbol{x},E)} \simeq A \quad , \tag{1.10}$$

where $S(\boldsymbol{x},E)$ is the external neutron source distribution function.

Function of neutron flux distribution from fission ϕ_f can be expressed as

$$\phi_\mathrm{f} = \Psi M \Psi_{0,L} S \quad , \tag{1.11}$$

where $(M\Psi_{0,L}S)$ corresponds to the neutrons which are generated by the fission reactions caused directly by the neutrons emitted from the external neutron source. By considering that $(M\Psi_{0,L}S)$ represents a neutron source,

$$\frac{\phi_\mathrm{f}(\boldsymbol{x},E)}{\varphi_0(\boldsymbol{x},E)} \simeq B \quad , \tag{1.12}$$

where B is another constant. Accordingly, k_eff is approximated as follows:

$$k_\mathrm{eff} = \frac{\langle M\phi_\mathrm{f}\rangle}{\langle L\phi_\mathrm{f}\rangle} \simeq \frac{\langle M\varphi_0\rangle}{\langle L\varphi_0\rangle} = \lambda_0 \quad . \tag{1.13}$$

Under the one point reactor approximation, every generation of neutrons is assumed to create the similar neutron flux distribution with the fundamental mode. The number of neutrons in each each generation forms a geometric series, whose sum is represented as follows:

$$\left\langle \frac{1}{v}\phi \right\rangle \simeq \frac{\langle S \rangle}{\bar{l}} \frac{1}{1-k_{\text{eff}}} \quad , \tag{1.14}$$

where $v(E)$ is the velocity of neutrons whose energy is E, and $\bar{l}$ the averaged neutron lifetime. As a result, count rate n of a neutron detector is approximated as

$$n \propto \frac{1}{1-k_{\text{eff}}} \quad , \tag{1.15}$$

where the proportional coefficient is independent of k_{eff}.

If the count rate of the neutron detector is obtained for a certain state where the subcriticality is known, then a one-to-one correspondence is established between the count rate and the subcriticality.

Dependence on the detector position

The one point reactor approximation of Eq. (1.9) is very rough, especially in the case of steady subcritical state with external neutron sources. The measurement results using Eq. (1.15) are dependent on the position of the neutron detector, since the relative neutron flux distribution is dependent on k_{eff}.[9)]

When macroscopic cross sections have changed in a certain region, R, the neutron flux distribution and k_{eff} change as well. The change of neutron flux is relatively small in the region near the external neutron source or far away from R. If the neutron detector is located in these regions, measurement results by the ordinary neutron source multiplication method with the one point reactor approximation underestimate the change of subcriticality. By contrast, if the neutron detector is located in R or far away from the external neutron source, the results may overestimate it. The measurement results are always inaccurate due to this intrinsic error in the one point reactor approximation.

1.3.2 Higher Mode Source Multiplication Method

As an improvement of the neutron source multiplication method, the higher mode source multiplication method has been proposed.[10)] The basic concept of this method is to expand the unknown neutron flux distribution function with the known eigenfunctions. By this expansion, the relative neutron flux distribution in the measured system is expected to be estimated more accurately than the case that the one point reactor approximation is applied. Consequently, the dependence of the measurement results on the detector positions may be reduced.

However, significant dependence on the detector position was observed as experimental results.[11,12] This dependence is caused by two inappropriate assumptions which are employed in the derivation of the higher mode source multiplication method. Furthermore, the original derivation did not define the exact meaning of the phrase of 'operators are uniform'. The derivation has been complemented as follows.

Derivation

The higher mode source multiplication method is based on the following approximation:

$$\phi' \simeq \sum_{i=0}^{\infty} C_i \varphi_i \quad , \tag{1.16}$$

where ϕ' is the neutron flux distribution function of the system being measured, which is called *measured system*, φ_i the i-th mode of the eigenfunctions of a known system, which is called *initial state* in this section, and C_i the expansion coefficient of i-th mode.

Adjoint creation and annihilation operators of the initial state, $M^\dagger$ and $L^\dagger$, respectively, are defined as operators which satisfy the following equations for any neutron flux distribution functions ϕ and ψ:

$$\left\langle M^\dagger \phi,\ \psi \right\rangle = \langle \phi,\ M\psi \rangle \quad , \tag{1.17}$$

and

$$\left\langle L^\dagger \phi,\ \psi \right\rangle = \langle \phi,\ L\psi \rangle \quad , \tag{1.18}$$

where M and L are the creation and annihilation operators of neutrons in the initial state. This definition is valid so far as the boundary condition is imposed on ϕ and ψ that the neutron flux is zero at infinite distance. Adjoint eigenfunctions $\varphi_i^\dagger$ are defined as the solution of the following equation:

$$L^\dagger \varphi_i^\dagger = \frac{1}{\lambda_i} M^\dagger \varphi_i^\dagger \quad , \tag{1.19}$$

where λ_i are eigenvalues of the initial state. The adjoint eigenfunctions can be normalized to satisfy the following orthogonality:

$$\left\langle \varphi_i^\dagger,\ M\varphi_j \right\rangle = \delta_{i,j} \quad , \tag{1.20}$$

where $\delta_{i,j}$ is the Kronecker delta.

The equation of the neutron equilibrium in the measured system is

$$L'\phi' = M'\phi' + S \quad , \tag{1.21}$$

where M' and L' are the creation and annihilation operators of neutrons in the measured system, and S represents the external neutron source distribution function. This equation can be expanded as

$$L\sum_{i=0}^{\infty} C_i\varphi_i - \Sigma_\Delta\phi' = M\sum_{i=0}^{\infty} C_i\varphi_i + S \quad , \tag{1.22}$$

$$\Sigma_\Delta \equiv (M'-M)-(L'-L) \quad . \tag{1.23}$$

The inner product of each term in Eq. (1.22) with $\varphi_j^\dagger$ satisfies the following relationship due to the orthogonality of Eq. (1.20):

$$\frac{1}{\lambda_j}C_j - \left\langle \varphi_j^\dagger,\ \Sigma_\Delta\phi' \right\rangle = C_j + \left\langle \varphi_j^\dagger,\ S \right\rangle \quad . \tag{1.24}$$

Under the assumption of

$$\Sigma_\Delta = RM \quad , \tag{1.25}$$

where R is a constant that

$$|R| \ll 1 \quad , \tag{1.26}$$

the following relation is obtained under the 1st order approximation:

$$\frac{1}{\lambda_i}-\frac{1}{\lambda_i'} = \frac{\left\langle \varphi_i^\dagger,\ L\phi' \right\rangle}{\left\langle \varphi_i^\dagger,\ M\phi' \right\rangle} - \frac{\left\langle \varphi_i^\dagger,\ L\phi' \right\rangle}{(1+R)\left\langle \varphi_i^\dagger,\ M\phi' \right\rangle} = \frac{R-R^2}{1-R^2}\frac{\left\langle \varphi_i^\dagger,\ L\phi' \right\rangle}{\left\langle \varphi_i^\dagger,\ M\phi' \right\rangle} \simeq (1-R)R\frac{\left\langle \varphi_i^\dagger,\ L\phi' \right\rangle}{\left\langle \varphi_i^\dagger,\ M\phi' \right\rangle} \quad , \tag{1.27}$$

where λ_i' are the eigenvalues in the measured system. R and C_i have, accordingly, the following relation:

$$\frac{1}{1-R}\left(\frac{1}{\lambda_i}-\frac{1}{\lambda_i'}\right) \simeq \frac{R\left\langle \varphi_i^\dagger,\ L\phi' \right\rangle}{\left\langle \varphi_i^\dagger,\ M\phi' \right\rangle} = \frac{1}{\lambda_i}\frac{\left\langle \varphi_i^\dagger,\ \Sigma_\Delta\phi' \right\rangle}{\left\langle \varphi_i^\dagger,\ M\phi' \right\rangle} = \frac{\left(\frac{1}{\lambda_i}-1\right)C_i - \left\langle \varphi_i^\dagger,\ S \right\rangle}{\lambda_i C_i} \quad , \tag{1.28}$$

and so

$$C_i \simeq \left\langle \varphi_i^\dagger,\ S \right\rangle \left\{ \left(\frac{1}{\lambda_i}-1\right) - \frac{\lambda_i}{1-R}\left(\frac{1}{\lambda_i}-\frac{1}{\lambda_i'}\right) \right\}^{-1} \quad . \tag{1.29}$$

$\phi'(\boldsymbol{x}, E)$ can be expanded as follows:

$$\phi' = \sum_{i=0}^{\infty} C_i\varphi_i \simeq \sum_{i=0}^{\infty} \frac{\left\langle \varphi_i^\dagger,\ S \right\rangle}{\left(\frac{1}{\lambda_i}-1\right) - (\lambda_i)^2 R}\varphi_i \quad . \tag{1.30}$$

The value of R can be calculated from the ratio of the count rates of the neutron detector between the initial state and the measured system, and then ϕ' is estimated.

Because of Eq. (1.25), function of neutron flux distribution from source ϕ_s is not changing. As a result, subcriticality $\Delta\rho$ can be calculated on the basis of definition. Furthermore, eigenvalues λ'_i are estimated as follows:

$$\frac{1}{\lambda'_i} \simeq \frac{1}{\lambda_i} - (1-R)R\frac{1}{\lambda_i} \simeq (1-R)\frac{1}{\lambda_i} \quad . \tag{1.31}$$

Incompleteness of eigenfunctions

Eigenfunctions do not form a complete set. As is implied in Appendix B, the discrepancy between $\phi'(\boldsymbol{x}, E)$ and $\left(\sum_{i=0}^{\infty} C_i \varphi_i(\boldsymbol{x}, E)\right)$ is usually large in the region nearby the external neutron source. This discrepancy may cause significant error on measurement results by the higher mode source multiplication method.

If the fuel region is lying between the external neutron source and the neutron detector, this discrepancy is, roughly, moderated by the fuel. As a result, the contribution by the incompleteness of eigenfunctions is reduced. By contrast, if the neutron detector is directly facing the external neutron source, the discrepancy invokes traumatic results.

Assumption of Eq. (1.25)

The assumption of Eq. (1.25) has been introduced just in order to transform the equations, without any theoretical bases. In real situations, this assumption can be rarely satisfied. For instance, when the density of the fuel is changed, Eq. (1.25) is invalid because L changes as well as M. In this case, the neutron flux distribution function cannot be estimated correctly, then significant error is caused. The error is extremely large if the neutron detector is placed near the region where the cross sections change.

Due to these two unreasonable assumptions, the higher mode source multiplication method can be effective only in some special cases.

1.3.3 Integral Versions and Modified Neutron Source Multiplication Method

The essence of the integral versions[13, 14] and the modified neutron source multiplication method[15–17] is to introduce corrections for the ordinary neutron source multiplication method with the one point reactor approximation, by using the adjoint eigenfunction of the measured system. However, there are no methods to measure the adjoint eigenfunctions accurately, so that the adjoint eigenfunctions of the measured systems are required to be estimated by the numerical calculation.

In terms of subcriticality monitoring, the geometry and the composition of the measured system should be assumed to be unknown. There is no way to calculate the adjoint eigenfunctions of unknown systems, thus these methods cannot be applied to the subcriticality monitoring.

1.4 Purpose of This Study: Consideration of the Number of Parameters

The essence of the neutron source multiplication method is to assume a one-to-one correspondence between the subcriticality and the count rates of detectors. The number of detectors is denoted by N in this paper. In exact discussion, there are an enormous number of parameters which contribute to the subcriticality. For instance, the nuclide composition of each fuel element is a respectively independent parameter. In order to find out the one-to-one correspondence, the number of parameters must be reduced to N or less by some approximations and assumptions. The way of this reduction dominates the accuracy of the measurement results.

In the case of the ordinary neutron source multiplication method with the one point reactor approximation, the subcriticality is assumed to be the only effective parameter in the system. This is, from another viewpoint, equivalent to the implicit assumption that no information on the system other than the count rates of the neutron detector is given to us. This assumption is too modest. In experiments, we have some information on the system, including the reactor size, the positions of the control rods, the initial composition of the fuel and reflector, and so on. This information should be taken into account for obtaining accurate results of the subcriticality measurement.

The higher mode source multiplication method is much more vigorous than using the one point reactor approximation. This method is based on the assumption that we know almost everything about the system, and only one parameter which is related to the subcriticality is unknown. This parameter is represented as R in Eq. (1.25). From the count rates of neutron detectors, R can be estimated, then coefficients C_i are estimated, and consequently the neutron flux distribution and the creation and annihilation operators are obtained as well. However, the application of the higher mode source multiplication method is very limited because the completeness of eigenfunctions and Eq. (1.25) are assumed.

The purpose of this study is to develop a new subcriticality measurement method, which can be applied to various systems without losing its theoretical consistency. The completeness of eigenfunctions is not assumed. As the basic assumption in this new method, results of numerical calculations are considered accurate. This method is aiming at obtaining the same result with the direct calculation of the measured system, while the exact geometry and composition of the system is unknown. For this aim, everything except N parameters which are related with the subcriticality is assumed to be known in the system. This means a generalization of the assumption of Eq. (1.25), in which R is the only unknown parameter.

This paper consists of the following 5 sections. The first one is the general discussion on the subcriticality measurement and the purpose of this study.

The derivation of the new method, which is named *imaginary source multiplication method*, is shown in Section 2. This new method is based on the concept of imaginary neutron source, which is proposed in this paper as well. The concept of imaginary neutron source is to treat the change of macroscopic cross sections as placement of a neutron source in the equation. The imaginary neutron source distribution function in the measured system can be estimated by numerical calculations for the initial state and the measurement results. No calculations on the measured system are required.

In order to examine the validity of the above theory, the agreement between the results of the imaginary source multiplication method and those of the direct calculations is demonstrated in Section 3, on the basis of diffusion calculation. The advantage over the conventional neutron source multiplication methods is shown as well. The imaginary source multiplication method can be applied to various systems without losing its accuracy.

In Section 4, an experimental weak point is shown. The imaginary source multiplication method requires accurate numerical calculations for the initial state, in order to estimate the imaginary neutron source distribution function. In other words, this method places full confidence in the results of the numerical calculation. The accuracy of the measurement results highly depend on that of the numerical calculation. If the numerical calculation is very inaccurate, the measurement results may have less accuracy than the conventional neutron source multiplication methods. In experiments, there always exist some discrepancy between the result of the numerical calculation and that of the measurement. This discrepancy appears as the measurement error in the results of the imaginary source multiplication method.

As the conclusion, by using the imaginary source multiplication method, the subcriticality can be accurately measured so far as the numerical calculation for the initial state is accurate enough.

§2 Theory of Imaginary Neutron Source

2.1 Definition of imaginary neutron source

The imaginary source multiplication method is based on the concept of imaginary neutron source. This concept is described in this section.

The basic concept of imaginary neutron source is to consider the change of macroscopic cross sections as a neutron source. For instance, when a control rod is inserted and the system has become a steady state, the control rod absorbs neutrons by a constant rate. This behaviour is considered as a result of introducing a neutron source with negative intensity. Then, the neutron flux distribution function of this system is understood as the sum of the two functions, namely one is the neutron flux distribution function with the real neutron source and no control rods, and one with the imaginary neutron source.

Definition

In a steady subcritical system with external neutron sources, it is assumed that the relative neutron flux distribution function and the macroscopic cross sections are known. This system is called *initial state* in this paper. The equation of the neutron equilibrium in this system is written as

$$L\phi_0 = M\phi_0 + S \quad , \tag{2.1}$$

where M and L are the creation and annihilation operators of neutrons in the initial state, respectively, ϕ_0 is the neutron flux distribution function, and S the external neutron source distribution function. The steady state after the creation and annihilation operators are changed into M' and L', respectively, is called *final state*. The equation of the neutron equilibrium in the final state is

$$L'\phi' = M'\phi' + S \quad , \tag{2.2}$$

where ϕ' is the neutron flux distribution function in the final state.

Imaginary neutron source distribution function I is defined as

$$I \equiv \Sigma_\Delta \phi' \quad , \tag{2.3}$$

$$\Sigma_\Delta \equiv (M' - M) - (L' - L) \quad , \tag{2.4}$$

so that

$$L\phi' = M\phi' + S + I \quad . \tag{2.5}$$

Since Eqs. (0.1), (2.1), and (2.2) have unique solutions respectively, the following relation is always valid:

$$\phi' = \phi_0 + \Psi I \quad . \tag{2.6}$$

This equation explains that the change of the neutron flux distribution from ϕ_0 to ϕ' can be considered to be caused by the placement of the imaginary neutron source represented by I, instead of the changes of the operators. By estimating I with some approximations, ϕ' can be calculated.

2.2 Imaginary Source Multiplication Method

2.2.1 Restriction Condition on the System

As is described in Section 1.4, the imaginary source multiplication method assumes that we know everything about the final state except N parameters, which are related with the subcriticality. This assumption is equivalent to that some approximations and assumptions must be already applied to the system in order to reduce the number of parameters to N. In this paper, this assumption is represented as a restriction condition that Σ_Δ can be expressed as a superposition of known operators $\Sigma_{\Delta j}$ as follows:

$$\Sigma_\Delta = \sum_{j=1}^{N} C_j \Sigma_{\Delta j} \quad , \tag{2.7}$$

where the j-th known operator $\Sigma_{\Delta j}$ is arbitrary, and C_j is the j-th coefficient whose value is unknown.

$\Sigma_{\Delta j}$ should be chosen based on the information that we have about the final state. For instance, when uniform reduction of fuel density in the whole system and increase of absorber density at a certain region occur simultaneously, $\Sigma_{\Delta 1}$ may represent the uniform change of a unit amount, while $\Sigma_{\Delta 2}$ corresponds to the unit amount of the latter one. The real amount of the change of cross sections is assumed to be unknown, and it is represented as unknown coefficients C_1 and C_2.

In the real situation, there are some cases, including control rod insertion and change of amount of liquid fuel, that cannot be represented as the restriction condition of Eq. (2.7). For handling these cases by the imaginary source multiplication method, rough approximations are employed such as regarding control rod insertion as change of absorber density.

2.2.2 *i*-th Order Imaginary Source Approximation

Imaginary neutron source distribution function I seen in Eq. (2.3) cannot be directly calculated, since unknown function ϕ' and unknown operator Σ_Δ are contained in this equation. A perturbation method which is different from the ordinary perturbation method of nuclear reactor physics is introduced.

k-th order imaginary neutron source distribution function $I^{(k)}$ is defined as

$$I^{(k)} \equiv \Sigma_\Delta \left(\Psi \Sigma_\Delta\right)^{k-1} \phi_0 \quad , \tag{2.8}$$

while the following approximation is named *i-th order imaginary source approximation*:

$$I \simeq \sum_{k=1}^{i} I^{(k)} \quad . \tag{2.9}$$

This definition comes from the following discussion. The 1st order imaginary source approximation is equivalent to the assumption that the neutron flux distribution is not changing between the initial state and the final state. As the first order approximation,

$$I \simeq I^{(1)} \quad , \tag{2.10}$$

$$\phi' \simeq \phi_0 + \Psi I^{(1)} \quad . \tag{2.11}$$

Then the 2nd order imaginary neutron source distribution function is defined for the correction for the second term of the right-hand side in Eq. (2.11):

$$I^{(2)} = \Sigma_\Delta \Psi I^{(1)} \quad , \tag{2.12}$$

so that

$$I \simeq \Sigma_\Delta \left(\phi_0 + \Psi I^{(1)} \right) = \sum_{k=1}^{2} I^{(k)} \tag{2.13}$$

is obtained as the second order approximation. Inductively, Eqs. (2.8) and (2.9) are obtained.

The convergence condition of $I^{(k)}$ is discussed in Section 2.2.3. If $I^{(k)}$ is convergent,

$$\lim_{i \to \infty} \sum_{k=1}^{i} I^{(k)} = I \quad , \tag{2.14}$$

is supposed, since

$$\lim_{i \to \infty} \sum_{k=1}^{i} I^{(k)} = \Sigma_\Delta \left(\phi_0 + \Psi \lim_{i \to \infty} \sum_{k=1}^{i} I^{(k)} \right) \quad , \tag{2.15}$$

which is the property of function I. In principle, I is not the only function which has this property. In other words, a certain function, denoted by f, may satisfy

$$I \neq f = \Sigma_\Delta \left(\phi_0 + \Psi f \right) \quad . \tag{2.16}$$

However, Ψf must have quite strange values as a neutron flux distribution function. Hence, being convergent is approximately considered as a sufficient condition of the relationship in Eq. (2.14).

By substituting Eq. (2.7) into Eqs. (2.8) and (2.9), I is transformed into

$$I \simeq \sum_{j=1}^{N} \sum_{k=1}^{i} C_j \Sigma_{\Delta j} \left(\sum_{l=1}^{N} C_l \Psi \Sigma_{\Delta l} \right)^{k-1} \phi_0 \quad . \tag{2.17}$$

By solving this equation of k-th degree of unknown variables C_j, the neutron flux distribution function in the final state can be estimated.

The function of neutron flux distribution from source can be estimated as well. The following equations correspond to Eqs. (2.6), (2.3), and (2.4), respectively:

$$\phi'_s = \phi_{s0} + \Psi_{0,L} I_s \quad , \tag{2.18}$$

$$I_s \equiv \Sigma_L \phi'_s \quad , \tag{2.19}$$

$$\Sigma_L \equiv -(L' - L) \quad , \tag{2.20}$$

where ϕ'_s is the function of neutron flux distribution from source in the final state, and ϕ_{s0} is that in the initial state. By i-th order imaginary source approximation, I_s can be estimated as follows:

$$I_s \simeq \sum_{k=1}^{i} \Sigma_L \left(\Psi_{0,L}\Sigma_L\right)^{k-1} \phi_{s0} \quad . \tag{2.21}$$

2.2.3 Convergence Condition

The exact derivation of the convergence condition of $I^{(k)}$, which is the i-th order imaginary neutron source distribution function, is too complicated. In this section, a roughly approximated convergence condition is discussed, by using the one point reactor approximation. The following relation is valid under the one point reactor approximation:

$$\phi(\boldsymbol{x}, E) = \frac{A(\boldsymbol{x}, E)}{1 - k_{\text{eff}}} \quad , \tag{2.22}$$

where ϕ is the neutron flux distribution function, and A a function which is independent from k_{eff}. The derivation of this equation was shown in Section 1.3.1.

Since functions ϕ and $(\Psi\Sigma_\Delta\phi)$ are assumed to be similar, operator $(\Psi\Sigma_\Delta)$ is equivalent to a coefficient, which is denoted by α in this section. k-th order imaginary neutron source distribution function satisfies

$$\Psi I^{(k)} = \alpha^k \phi_0 \quad . \tag{2.23}$$

The convergence condition of $I^{(k)}$ is consequently

$$|\alpha| < 1 \quad . \tag{2.24}$$

The relationship of the neutron flux distribution functions between the initial state and the final state is

$$\phi' = \phi_0 + \sum_{k=1}^{\infty} \Psi I^{(k)} = \frac{1}{1-\alpha}\phi_0 \quad . \tag{2.25}$$

Inequation (2.24) is equivalent to

$$\phi'(\boldsymbol{x}, E) > \frac{1}{2}\phi_0(\boldsymbol{x}, E) \quad . \tag{2.26}$$

Under the one point reactor approximation, this inequation is transformed into

$$1 - k' < 2\,(1 - k_0) \quad , \tag{2.27}$$

where k' and k_0 are the effective multiplication factors in the final and initial states, respectively. Inequation (2.27) represents the roughly approximated condition of the convergence. The initial state should be chosen to satisfy this condition.

2.2.4 Estimation of Subcriticality

In order to solve Eq. (2.17), the conversion factor between the measured count rate and the calculated reaction rate is required. This factor can be determined at any arbitrary known subcritical system, since it is supposed to be independent from the geometry and the composition. This known system is called *calibration system* in this paper.

Detection efficiency ε_l of the l-th neutron detector is defined as follows:

$$\varepsilon_l = \frac{n_l}{\displaystyle\int \Sigma_d(E)\phi(\boldsymbol{x}_l, E)\ \mathrm{d}E} \quad , \tag{2.28}$$

where n_l is the count rate, Σ_d the macroscopic cross section of the reaction used by the neutron detector, ϕ the neutron flux distribution function, and $\boldsymbol{x}_l$ the neutron detector position.

The following equation of unknown variables C_j, which are included in $I^{(k)}$, is obtained by the assumption that the detection efficiency is unchanged throughout the experiment:

$$\frac{n'_l}{n_{cl}} = \frac{\displaystyle\int \Sigma_d \left(\phi_0(\boldsymbol{x}_l, E) + \sum_{k=1}^{i} \Psi I^{(k)}(\boldsymbol{x}_l, E)\right)\ \mathrm{d}E}{\displaystyle\int \Sigma_d \phi_c(\boldsymbol{x}_l, E)\ \mathrm{d}E} \quad , \tag{2.29}$$

where n'_l and n_{cl} are the count rates of l-th detector in the final state and the calibration system, respectively, and ϕ_c is the neutron flux distribution function in the calibration system.

Using a steady critical state as the calibration system without the external neutron sources is possible as well. The advantage of using a steady critical state instead of a subcritical state is that neutron flux distributions in the critical states can be calculated more accurately than those in the subcritical states.

From the count rate of each neutron detector in the calibration system, relative detection efficiency $\frac{\varepsilon_l}{\varepsilon_0}$ between the 0th and l-th neutron detectors is obtained as follows:

$$\frac{\varepsilon_l}{\varepsilon_0} = \frac{n_{cl}\left(\int \Sigma_d(E)\phi_c(\boldsymbol{x}_l, E)\ \mathrm{d}E\right)^{-1}}{n_{c0}\left(\int \Sigma_d(E)\phi_c(\boldsymbol{x}_0, E)\ \mathrm{d}E\right)^{-1}} \quad . \tag{2.30}$$

In the final state, the following equation is valid when i is large enough:

$$\frac{n'_l}{n'_0} = \frac{\varepsilon_l \int \Sigma_d(E)\left(\phi_0(\boldsymbol{x}_l, E) + \sum_{k=1}^{i}\sum_{j=1}^{N} C_j^k \Psi I^{(k)}(\boldsymbol{x}_l, E)\right)\ \mathrm{d}E}{\varepsilon_0 \int \Sigma_d(E)\left(\phi_0(\boldsymbol{x}_0, E) + \sum_{k=1}^{i}\sum_{j=1}^{N} C_j^k \Psi I^{(k)}(\boldsymbol{x}_0, E)\right)\ \mathrm{d}E} \quad . \tag{2.31}$$

For instance, the following equation is obtained under the 1st order imaginary source approximation:

$$\frac{n'_l}{n'_0} = \frac{\varepsilon_l \int \Sigma_d(E)\phi_0(\boldsymbol{x}_l, E)\ \mathrm{d}E + \varepsilon_l \sum_{j=1}^{N} C_j \int \Sigma_d(E)\Psi\Sigma_{\Delta j}\phi_0(\boldsymbol{x}_l, E)\ \mathrm{d}E}{\varepsilon_0 \int \Sigma_d(E)\phi_0(\boldsymbol{x}_0, E)\ \mathrm{d}E + \varepsilon_0 \sum_{j=1}^{N} C_j \int \Sigma_d(E)\Psi\Sigma_{\Delta j}\phi_0(\boldsymbol{x}_0, E)\ \mathrm{d}E} \quad . \tag{2.32}$$

By using $(N+1)$ neutron detectors, N simultaneous equations are obtained. C_j can be estimated by solving the simultaneous equations of (2.29) or (2.31). The neutron flux distribution in the final state can be calculated by using Eqs. (2.9), (2.8) and (2.21). One of the advantages of this method is that no numerical calculations other than solving the simultaneous equations are required after the detection of neutrons. We do not need to wait long time during the calculation.

The creation and annihilation operators and the function of neutron flux distribution from source in the final state can be estimated as well as the neutron flux distribution function. Hence, the subcriticality in the final state can be calculated by the following definitions:

$$\Delta\rho = 1 - \frac{1}{k_{\text{eff}}} \quad , \tag{2.33}$$

$$k_{\text{eff}} = 1 - \frac{\langle M'\phi'_s\rangle}{\langle M'\phi'\rangle} \quad . \tag{2.34}$$

2.2.5 Requirements for the Imaginary Source Multiplication Method

The concept of imaginary neutron source makes it possible to estimate the subcriticality without requiring any special conditions on the measured system. The primitive implementation of the imaginary source multiplication method described in this paper requires the following conditions: 1) the operators in the initial state are known, 2) the neutron flux distribution function in the initial state is known, and 3) the origin of the change of cross sections is known, namely Eq. (2.7) must be satisfied.

The most important point about condition 3) is that the origin must be known qualitatively, but the exact amount of the change may not be known. Furthermore, this condition is not essential. Another implementation of the imaginary source multiplication method is considered to be possible without using this condition. For instance, when the volume of fuel solution is changed by unknown amount, Eq. (2.7) cannot be satisfied. Even in this case, the number of parameters is only one, namely the volume of fuel solution. Thus no other restriction conditions are required in principle.

In order to carry out the i-th order imaginary source multiplication method, the following functions are required to be calculated:

- Neutron flux distribution function in the initial state ϕ_0,
- Function of neutron flux distribution from source in the initial state ϕ_{s0},
- Functions $\Psi\Sigma_{\Delta j_1}\phi_0, \quad \Psi\Sigma_{\Delta j_2}\Psi\Sigma_{\Delta j_1}\phi_0, \quad \cdots, \quad \Psi\Sigma_{\Delta j_i}\cdots\Psi\Sigma_{\Delta j_1}\Psi_0 \qquad (j_x = 1, 2, \cdots, N)$,
- Functions $\Psi\Sigma_{L j_1}\phi_{s0}, \quad \Psi\Sigma_{L j_2}\Psi\Sigma_{L j_1}\phi_{s0}, \quad \cdots, \quad \Psi\Sigma_{L j_i}\cdots\Psi\Sigma_{L j_1}\Psi_{s0} \qquad (j_x = 1, 2, \cdots, N)$.

2.3 Correction for the Effect of the Higher Order Imaginary Neutron Source

In order to estimate the change of cross sections by the imaginary source multiplication method, high orders of the imaginary neutron source should be taken into account. If the calculation for the imaginary neutron sources consumes a large amount of computer resource, it is hard to calculate such high orders of the imaginary neutron source. In this case, the contribution of the higher orders of the imaginary neutron source can be approximately taken into account by some corrections.

Under the i-th order imaginary source approximation, the imaginary neutron source distribution function is approximated as follows:

$$\sum_{k=1}^{i} I^{(k)} \simeq I = \Sigma_\Delta \left(\phi_0 + \Psi I\right) \simeq \Sigma_\Delta \left(\phi_0 + \Psi \sum_{k=1}^{i} I^{(k)}\right) \quad . \tag{2.35}$$

On the other hand, the following equation is obtained by definition:

$$\sum_{k=1}^{i} I^{(k)} = \Sigma_\Delta \left(\phi_0 + \Psi \sum_{k=1}^{i-1} I^{(k)}\right) \quad , \tag{2.36}$$

which is equivalent to Eq. (2.8). By these equations, the i-th order imaginary source approximation is considered to be based on the following assumption:

$$I^{(i)} \sim 0 \quad . \tag{2.37}$$

This assumption may cause significant errors when i is not large enough.

In order to avoid these errors, the i-th order imaginary source approximation in Eq. (2.35) is modified by introducing correction factor R_i as follows:

$$R_i \sum_{k=1}^{i} I^{(k)} \simeq I \simeq \Sigma_\Delta \left(\phi_0 + R_i \Psi \sum_{k=1}^{i} I^{(k)}\right) \quad . \tag{2.38}$$

From Eqs. (2.36) and (2.38), R_i is approximated as

$$R_i \simeq \left(1 - \frac{\Sigma_\Delta \Psi I^{(i)}}{\Sigma_\Delta \phi_0}\right)^{-1} \quad . \tag{2.39}$$

R_i is defined as a real number which is independent of the position, while the value of the right-hand side in this equation is dependent on the position and the energy. R_i is approximately calculated by the integral as

$$R_i \simeq \left(1 - \frac{\langle \Sigma_\Delta \Psi I^{(i)} \rangle}{\langle \Sigma_\Delta \phi_0 \rangle}\right)^{-1} \quad . \tag{2.40}$$

By the i-th order imaginary source approximation,

$$\left\langle \Sigma_\Delta \Psi I^{(i)} \right\rangle = \left\langle I^{(i+1)} \right\rangle \ll \left\langle I^{(1)} \right\rangle = \langle \Sigma_\Delta \phi_0 \rangle \quad , \tag{2.41}$$

hence Eq. (2.40) is transformed into

$$R_i \simeq 1 + \frac{\left\langle \Sigma_\Delta \Psi I^{(i)} \right\rangle}{\langle \Sigma_\Delta \phi_0 \rangle} \quad . \tag{2.42}$$

By introducing R_i, Eq. (2.29) is modified as follows:

$$\frac{n'_l}{n_{cl}} = \frac{\displaystyle\int \Sigma_d \left(\phi_0(\boldsymbol{x}_l, E) + R_i \sum_{k=1}^{i} \Psi I^{(k)}(\boldsymbol{x}_l, E) \right) \, \mathrm{d}E}{\displaystyle\int \Sigma_d \phi_c(\boldsymbol{x}_l, E) \, \mathrm{d}E} \quad . \tag{2.43}$$

Simultaneous equations (2.42) and (2.43) can be numerically solved.

The transformation of Eq. (2.40) into Eq. (2.42) is unfair. This transformation is based on the assumption of inequation (2.41), but R_i was introduced because $\left\langle I^{(i+1)} \right\rangle$ is not negligible. However, as is shown in Section 3.2.3, some errors are observed when Eq. (2.40) is used instead of Eq. (2.42). This transformation is supposed to be necessary.

§3 Verification of the Consistency of the Theory

3.1 Calculation System

Numerical verifications of the theory for the imaginary source multiplication method have been performed. The verification has been conducted in 2-dimensional and 2-group diffusion calculation by SRAC2003[18] CITATION[19] code with JENDL-3.3.[20] The calculation system was divided into 164 × 176 grids, and no buckling was employed. The calculation system was composed of a 93 % highly enriched uranium solution surrounded by the light water reflector, as shown in Fig. 3.1. The nuclide composition is shown in Table 3.1. The largest eigenvalue in the initial state was $\lambda_0 = 0.9892$. All the neutron detectors are assumed to detect only thermal neutrons.

In the cases of ($N = 1$), Eq. (2.29) was solved by Newton's method. When ($N \geqq 2$), Eq. (2.29) becomes simultaneous equations, which were solved by the steepest descent method.

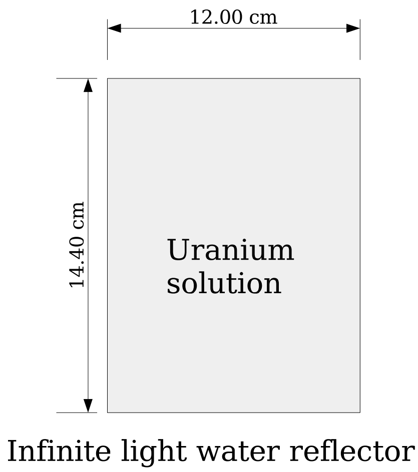

Fig. 3.1 Calculation system.

Table 3.1 Composition of the calculation system

Region	Nuclide	Number Density $[10^{24}\text{cm}^{-3}]$
Fuel	^{234}U	1.1257×10^{-5}
	^{235}U	1.5134×10^{-3}
	^{236}U	5.0147×10^{-6}
	^{238}U	9.3676×10^{-5}
	^{1}H	6.6615×10^{-2}
	^{2}H	7.6616×10^{-4}
	^{16}O	3.3312×10^{-2}
Reflector	^{1}H	6.6615×10^{-2}
	^{2}H	7.6616×10^{-4}
	^{16}O	3.3312×10^{-2}

3.2 Confirmation of the validity of the Imaginary Source Multiplication Method

3.2.1 Concept of the Imaginary Neutron Source

In this section, the validity of the concept of the imaginary neutron source is to be confirmed. In the initial state, an external fast neutron source was placed at position A shown in Fig. 3.2, and the fuel region was homogeneous. In the final state, the values of Σ_a and $\nu\Sigma_f$ were reduced by 18 % and 36 % in region B, respectively. Imaginary neutron source distribution function I was directly calculated by Eqs. (2.3) and (2.4). Here, operator Σ_Δ is represented as the following matrices:

$$\Sigma_\Delta = \begin{cases} \begin{pmatrix} -0.36\nu\Sigma_{f1} + 0.18\Sigma_{a1} & -0.36\nu\Sigma_{f2} \\ 0 & 0.18\Sigma_{a2} \end{pmatrix} & \text{(inside region } B\text{)} \\ \begin{pmatrix} 0 & 0 \\ 0 & 0 \end{pmatrix} & \text{(outside region } B\text{)} \end{cases}, \tag{3.1}$$

where neutron flux distribution functions are expressed as vertical vectors, ν is the mean number of produced neutrons per fission, and Σ_{fi} and Σ_{ai} are the macroscopic fission and absorption cross sections in the initial state for the i-th group, respectively.

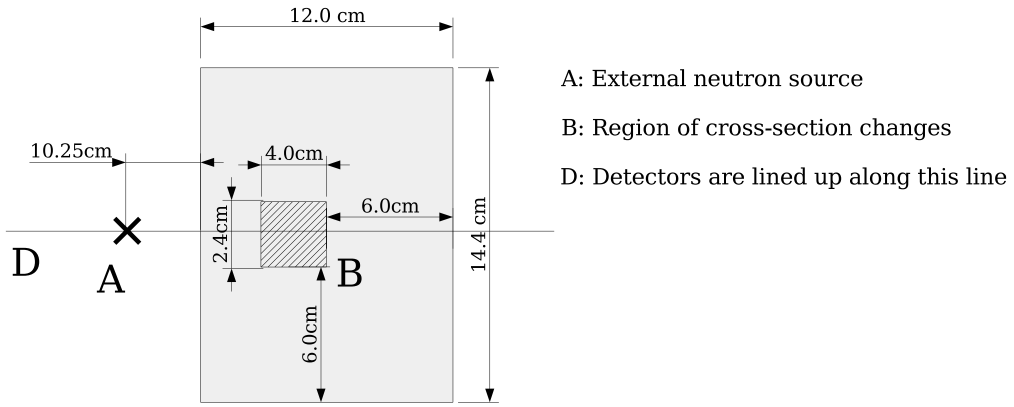

Fig. 3.2 Calculation system employed for the confirmation of the concept of imaginary neutron source

Figures 3.3 and 3.4 show the validity of the concept of imaginary neutron source. The solid vertical lines in these figures show the fuel region, the broken lines the region of cross section change, B, and the dotted lines the position of the external neutron source, A. The plotted lines and points are the values of functions $\phi_0, \phi', -\Psi\Sigma_\Delta\phi'$, and $\phi_0 + \Psi\Sigma_\Delta\phi'$, along line D in Fig. 3.2. The following relation, which comes from Eqs. (2.3), (2.4), and (2.5), has been confirmed by the overlap of the square marks and cross ones:

$$\phi' = \phi_0 + \Psi\Sigma_\Delta\phi' \quad . \tag{3.2}$$

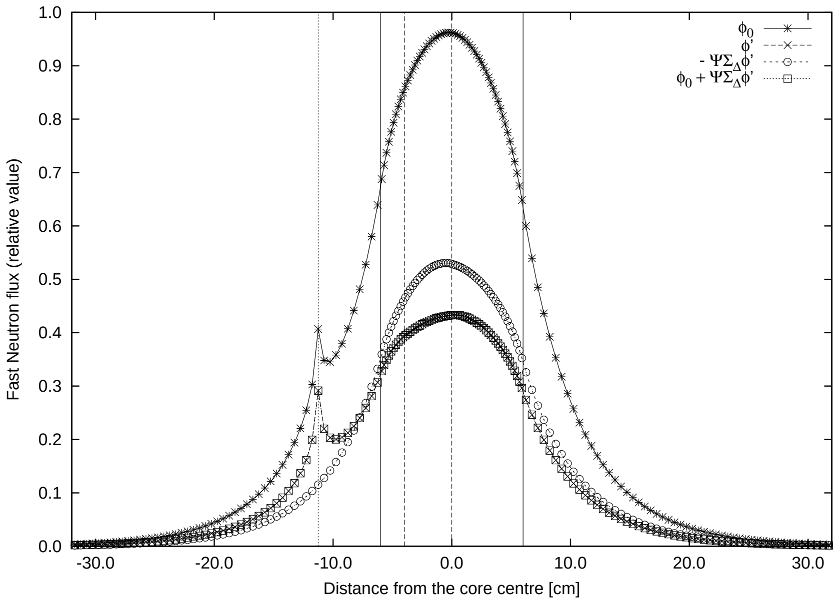

Fig. 3.3 Confirmed agreement of the fast neutron flux distributions. (Solid vertical lines: fuel region, broken lines: region of cross section change, dotted line: the external neutron source.)

As a result, the validity of the concept of imaginary neutron source has been verified. When the imaginary neutron source distribution function is accurately estimated, the neutron flux distribution function can be estimated as well. The subcriticality can be consequently estimated.

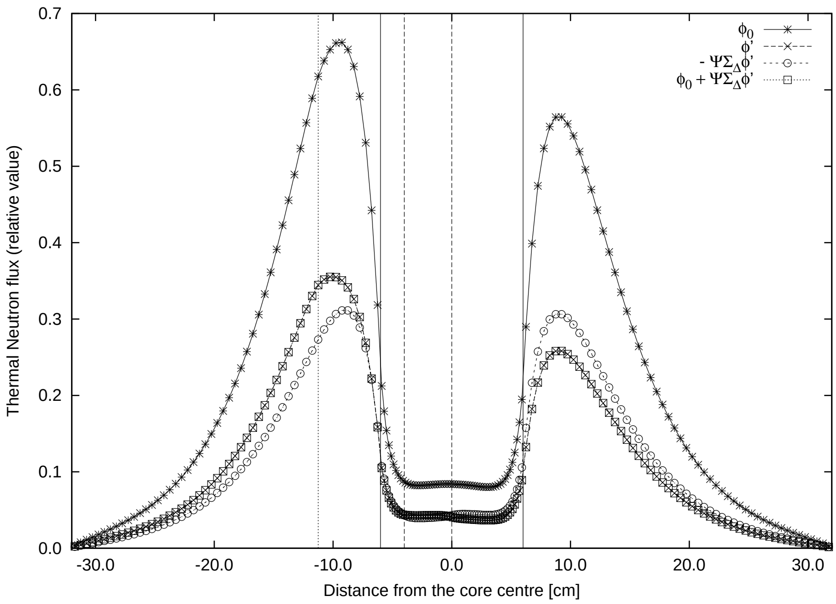

Fig. 3.4 Confirmed agreement of the thermal neutron flux distributions.

3.2.2 Exact Imaginary Source Multiplication Method

This section shows the possibility of subcriticality measurement by the imaginary source multiplication method. The imaginary source multiplication method has been applied to the similar system with Section 3.2.1, but the values of Σ_a and $\nu\Sigma_f$ of the final state were reduced from those of the initial state by 15 % and 30 %, respectively. The correction with factor R_i was not applied. The known operator $\Sigma_{\Delta 1}$ was defined as the following matrices:

$$\Sigma_{\Delta 1} \equiv \begin{cases} \begin{pmatrix} -\nu\Sigma_{f1} + \dfrac{1}{2}\Sigma_{a1} & -\nu\Sigma_{f2} \\ 0 & \dfrac{1}{2}\Sigma_{a2} \end{pmatrix} & \text{(in region } B\text{)} \\ \begin{pmatrix} 0 & 0 \\ 0 & 0 \end{pmatrix} & \text{(not in region } B\text{)} \end{cases} \tag{3.3}$$

Operator Σ_Δ satisfies the following relation:

$$\Sigma_\Delta = C_1 \Sigma_{\Delta 1} \quad , \tag{3.4}$$

where

$$C_1 = 3.000 \times 10^{-1} \quad . \tag{3.5}$$

The value of C_1 was assumed to be unknown.

Figure 3.5 shows the calculation results by the 1st order imaginary source multiplication method, shown as '1st order ISM method', and the ordinary neutron source multiplication method with the one point reactor approximation. The solid horizontal line shows the value of directly calculated subcriticality, $-2.265\%\frac{\Delta k}{k}$. Neutron detectors are assumed to be lined up along line D shown in Fig. 3.2, then the estimated subcriticality was plotted in Fig. 3.5.

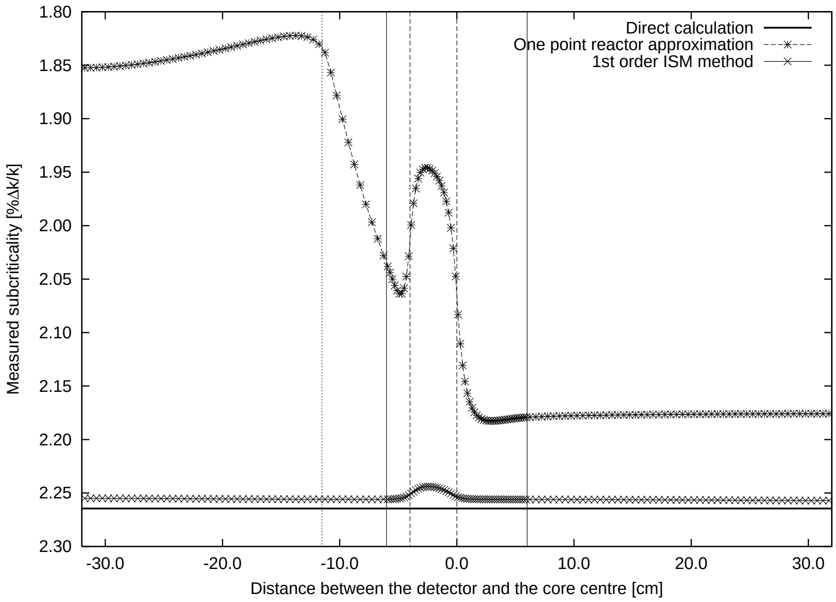

Fig. 3.5 Results obtained by the one point reactor approximation and the 1st order imaginary source approximation in comparison with the direct calculation.

The measurement results by the ordinary neutron source multiplication method with the one point reactor approximation are found to be inaccurate. The significant dependence of measurement results on the detector positions have been observed in Fig. 3.5. In the region on the left side of the external neutron source, the subcriticality is relatively underestimated, since the change in neutron flux is relatively small. Wherever the neutron detector is placed, the measurement results disagree with the result of direct calculation. By contrast, the measurement results by the 1st order imaginary source multiplication method includes only $0.021\%\frac{\Delta k}{k}$ of error at most. Theses results indicate that the 1st order imaginary source approximation can take account of the change in the neutron flux distribution accurately. The origin of this improvement in accuracy is that we have taken account of the information that the operators for the final state can be expressed as

$$M' - L' = (M - L) + C_1 \Sigma_{\Delta 1} \quad , \tag{3.6}$$

where C_1 is the only unknown parameter.

Figure 3.6 shows the dependence of the measurement results on the number of orders of the imaginary neutron source taken into account. The neutron detector was assumed to be placed next to the external neutron source. The solid curve shows the cases of odd numbers of i, while the broken curve represents the cases of even i. By increasing i, the estimated subcriticality converges on $-2.265\%\frac{\Delta k}{k}$, which agrees with the directly calculated value.

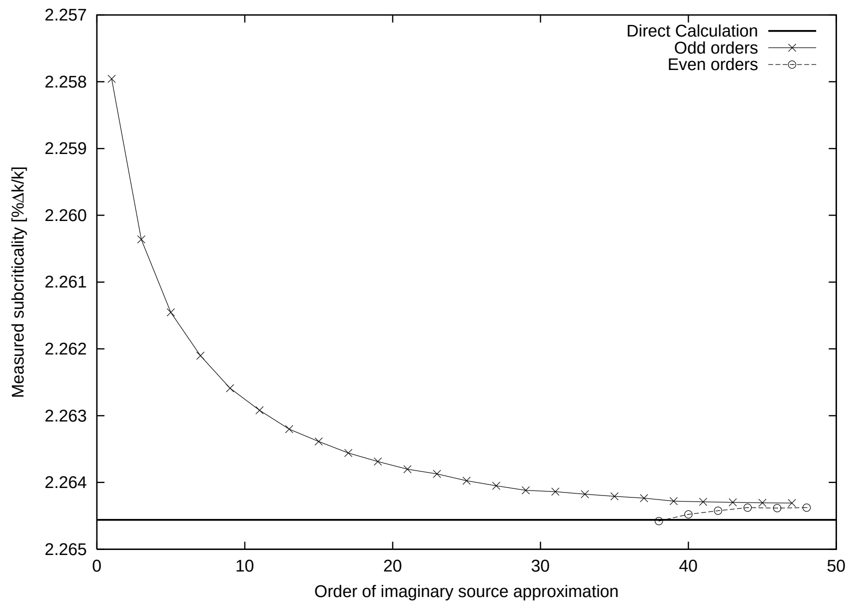

Fig. 3.6 Convergent behaviour of the imaginary source multiplication method.

When i is even and less than 38, Eq. (2.29) does not have real solutions. For instance, when $i = 2$, $(C_1)^3\,\Psi I^{(3)}$ is assumed to be negligible, so that $\phi'(\boldsymbol{x}, E)$ is approximated as

$$\phi'(\boldsymbol{x}, E) \simeq \phi_0 + C_1 \Psi I^{(1)}(\boldsymbol{x}, E) + (C_1)^2\,\Psi I^{(2)}(\boldsymbol{x}, E) \quad . \tag{3.7}$$

When $\phi'(\boldsymbol{x}, E)$ is considered as a function of C_1, the right-hand side in Eq. (3.7) has a minimum value while $\phi'(\boldsymbol{x}, E)$ does not have the minimum. Hence, if the measured count rate corresponds to the value of $\phi'(\boldsymbol{x}, E)$ which is less then the minimum value, there are no solutions of C_1.

Figure 3.7 shows the estimated values of C_1, which represents the amount of the change of the cross sections. The estimated values have exponentially converged on the correct value.

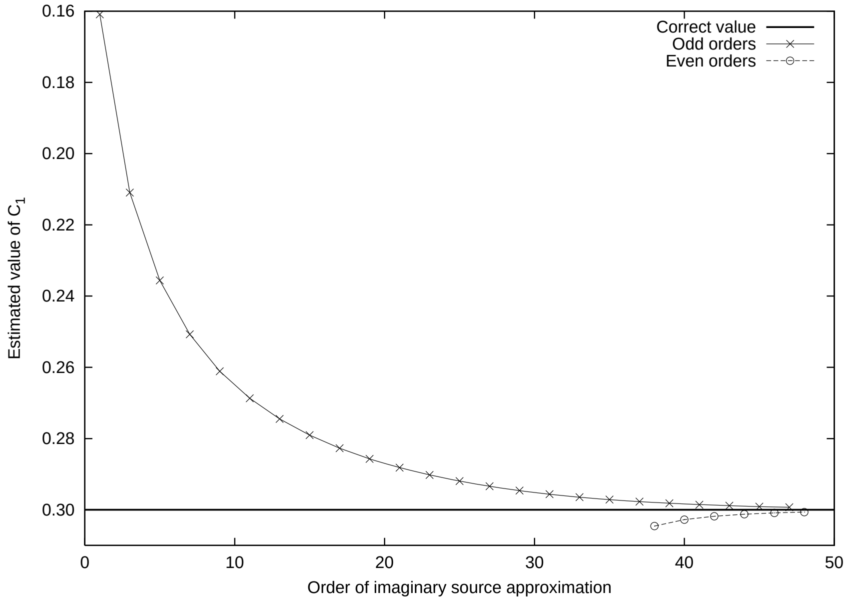

Fig. 3.7 Estimated values of C_1 when $C_1 = 0.30$.

The required value of i for convergence is dependent on the system. When there is less difference between the initial state and the final state, the convergence becomes faster. For instance when $C_1 = 2.400 \times 10^{-1}$, Eq. (2.29) had real solutions except the cases that i is even and less than 12. In addition, the estimation error of the values of C_1 were less than 1×10^{-3} when $i \geqq 24$, as shown in Fig. 3.8.

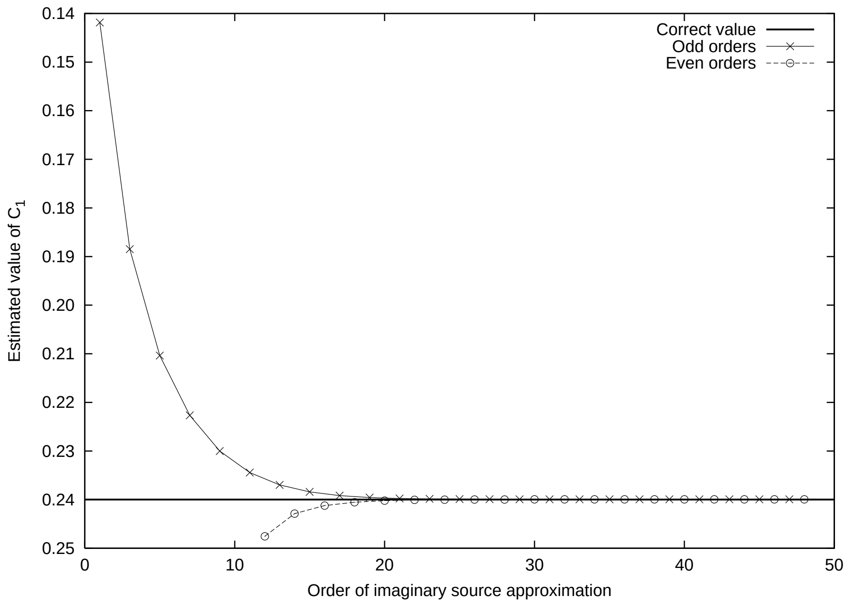

Fig. 3.8 Estimated values of C_1 when $C_1 = 0.24$.

3.2.3 Correction with $\boldsymbol{R_i}$

In contrast with the exact imaginary source multiplication method mentioned above, the estimated values of C_1 by using the correction with factors R_i are expected to converge rapidly. Simultaneous equations (2.42) and (2.43) were solved by the iteration calculation. The initial guess of R_i, which is denoted by $R_i^{(0)}$, was defined as

$$R_i^{(0)} \equiv 1.0 \quad . \tag{3.8}$$

Then $R_i^{(l)}$ where l are natural numbers are defined as

$$R_i^{(l)} \equiv 1 + \frac{\left\langle \Sigma_\Delta \Psi I^{(i)} \right\rangle}{\left\langle \Sigma_\Delta \phi_0 \right\rangle} \quad , \tag{3.9}$$

where Σ_Δ is obtained as the solution of the following simultaneous equations:

$$\frac{n_l'}{n_{cl}} = \frac{\displaystyle\int \Sigma_d \left(\phi_0(\boldsymbol{x}_l, E) + R_i^{(l-1)} \sum_{k=1}^{i} \Psi I^{(k)}(\boldsymbol{x}_l, E) \right) \, \mathrm{d}E}{\displaystyle\int \Sigma_d \phi_c(\boldsymbol{x}_l, E) \, \mathrm{d}E} \quad . \tag{3.10}$$

$R_i^{(l)}$ is supposed to converge on the correct value of R_i.

Figure 3.9 shows the estimated values of C_1 by the exact imaginary source multiplication method and those with the correction with R_i. The results with the correction were much more accurate than those of the exact imaginary source multiplication method. The error of the value of the estimated C_1 was less than 2×10^{-3} even in the case of the 1st order imaginary source approximation.

In contrast with the change of cross sections, the estimated neutron flux distribution by using the correction with R_i is not accurate. Figure 3.10 compares the estimated subcriticality by the exact imaginary source multiplication method and that by using the correction with R_i. In many cases, the correction leads to worse results, since the correction concentrates on the integration of the imaginary neutron source distribution function, as Eq. (2.42), and ignores the fine distribution.

Therefore, by combining the estimated neutron flux distribution by the exact imaginary source multiplication method and the estimated change of cross sections by using the correction with R_i, the subcriticality can be estimated more accurately as shown in Fig. 3.11.

As is mentioned before, the transformation of Eq. (2.40) into Eq. (2.42) is mathematically invalid. However, if Eq. (2.40) is used instead of Eq. (2.42), the accuracy of estimation of C_i is reduced, as shown in Fig. 3.12.

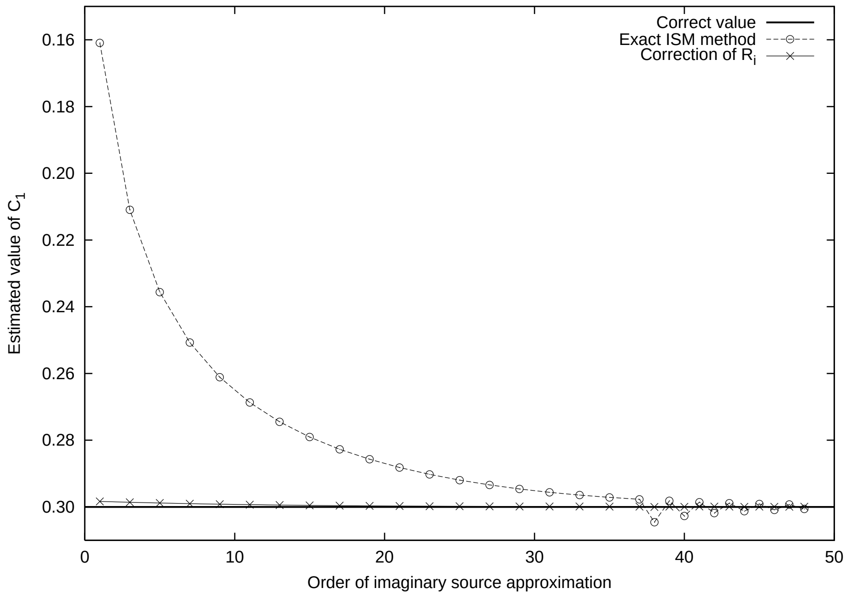

Fig. 3.9 Estimated values of C_1 by using the correction with R_i in comparison with those by the exact imaginary source multiplication method.

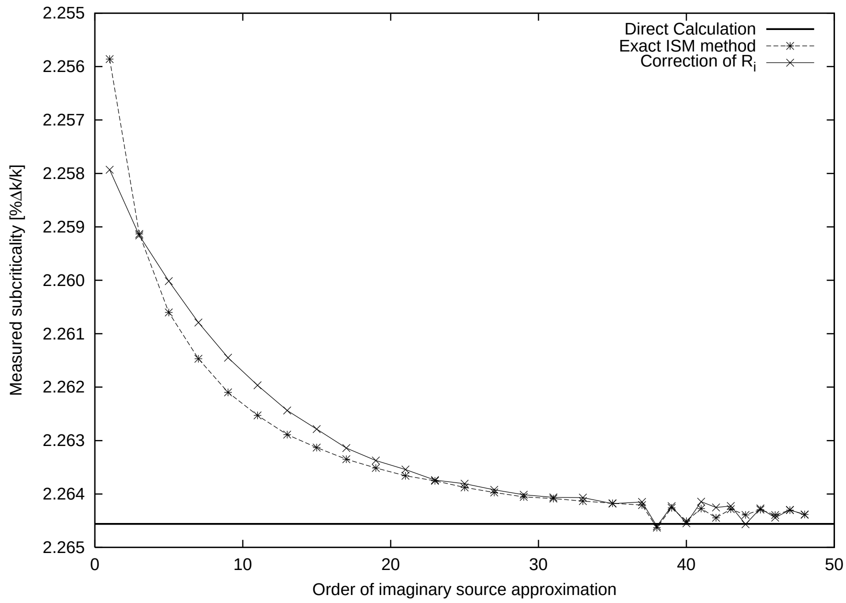

Fig. 3.10 Estimated subcriticality by using the correction with R_i in comparison with those by the exact imaginary source multiplication method.

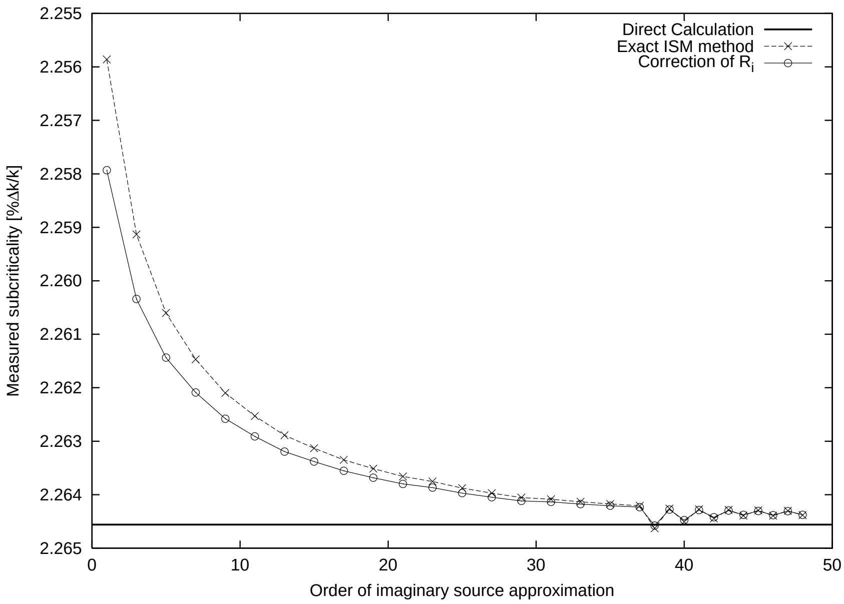

Fig. 3.11 Estimated subcriticality when R_i is applied only for the estimation of the change of cross sections.

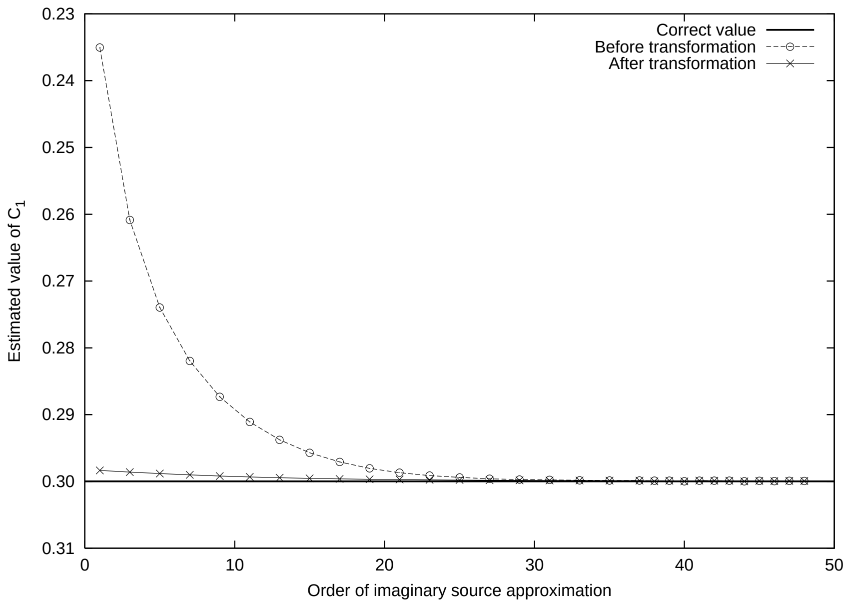

Fig. 3.12 Comparison of the estimation of C_i before and after the transformation of Eq. (2.40) into Eq. (2.42).

3.3 Advantages over the Higher Mode Source Multiplication Method

As is mentioned in Section 1.4, the imaginary source multiplication method is regarded as a generalized method of the higher mode source multiplication method. As the advantage of this generalization, the imaginary source multiplication method can be applied to various systems without losing its theoretical consistency. This advantage over the higher mode source multiplication method is numerically investigated in this section.

3.3.1 The Successful Case of the Higher Mode Source Multiplication Method

The discussion in Section 1.3.2 resulted in that the higher mode source multiplication method is based on two inappropriate assumptions, namely the possibility of the expansion of the neutron flux distribution function with the eigenfunctions, and Eq. (1.25). This section shows that the higher mode source multiplication method is effective when these two assumptions have been satisfied.

A hypothesis is propounded. The neutron flux distribution function can be expanded with the when the external neutron source is placed in the homogeneous fuel region and it has a similar spectrum with the fission spectrum. The grounds of this hypothesis are the necessary conditions of the expansion discussed in Appendix B and that eigenfunctions in the homogeneous fuel region is similar to cosine function, which forms a complete set. Based on this hypothesis, when a fast external neutron source is placed at position C shown in Fig. 3.13 and the subcriticality is changed by reducing $\nu\Sigma_f$ uniformly in the fuel region, the assumptions of the higher mode source multiplication method are supposed to be satisfied.

The value of $\nu\Sigma_f$ is reduced by 1 % so that the largest eigenvalue in the final state is 0.9793. The higher mode source multiplication method taking account up to the 200th expansion mode has been applied. Neutron detectors are assumed to be lined up along line D shown in Fig. 3.13, as well as the previous section. The eigenvalues and eigenfunctions in the initial state are calculated by NEUMAC-3 code.[21] The results of calculation of the value of $\left(1 - \dfrac{1}{\lambda_0'}\right)$ where λ_0' is the largest eigenvalue in the final state are shown in Fig. 3.14. The results of the higher mode source multiplication method are shown as 'Higher mode NSM method'. The value of the vertical axis, $\left(1 - \dfrac{1}{\lambda_0'}\right)$, is usually called subcriticality. However, the unit is % instead of $\%\frac{\Delta k}{k}$, since another definition of effective multiplication factor is

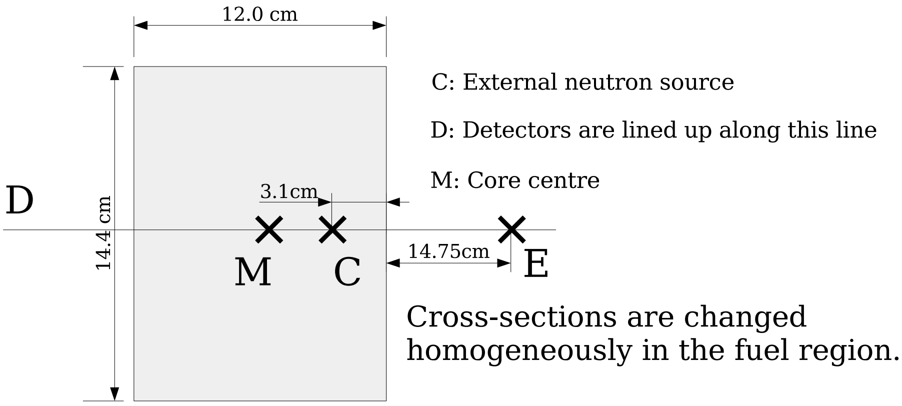

Fig. 3.13 Calculation system for the successful case of the higher mode source multiplication method

employed in this paper.

The results by the higher mode source multiplication method are quite accurate and almost no dependence on the detector position is observed. The error from the directly calculated value, −2.111%, is less than 0.001% except for the cases that the detector is placed close to the external neutron source. This agreement between the estimation and the direct calculation comes from the fact that the higher mode source multiplication method can accurately estimate the neutron flux distribution in the final state.

Figure 3.15 shows that the estimated neutron flux distribution agrees with the direct calculation where the neutron detector is placed at position E. Both distributions agree well except for the region nearby the external neutron source, which is represented by the dotted line. This disagreement around the external neutron source is merely caused by the insufficient number of the expansion modes taken into account. Figure 3.16 shows the dependence of the estimated neutron flux distribution on the number of the expansion modes. For increasing the number of expansion modes taken into account, the estimated neutron flux distribution becomes more accurate. Figure 3.17 shows the dependence of the measurement results on the number of the expansion modes taken into account. When the number of the expansion modes is small, the measurement results are inaccurate especially when the neutron detector is placed nearby the external neutron source.

As a conclusion, the higher mode source multiplication method is considered effective when the

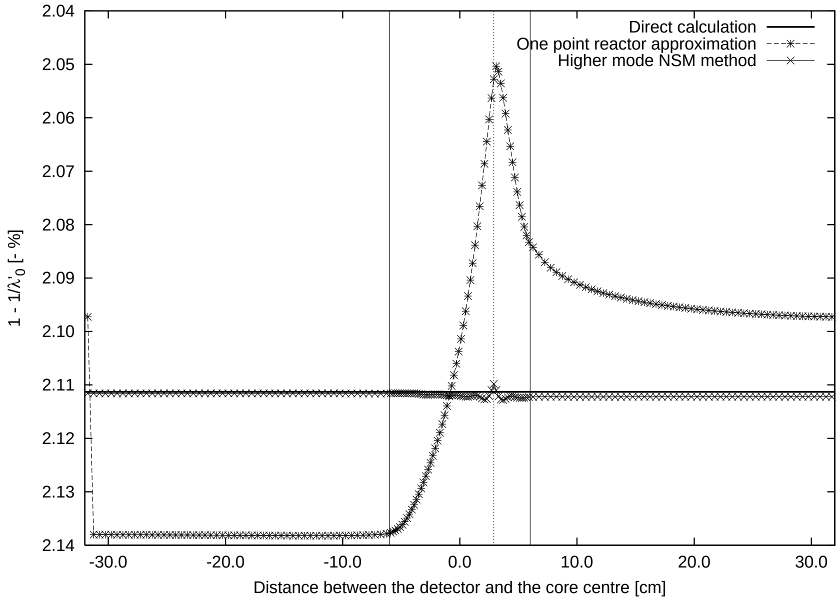

Fig. 3.14 A successful case of the higher mode source multiplication method for the estimation of subcriticality. (Solid vertical lines: fuel region, dotted line: the external neutron source.)

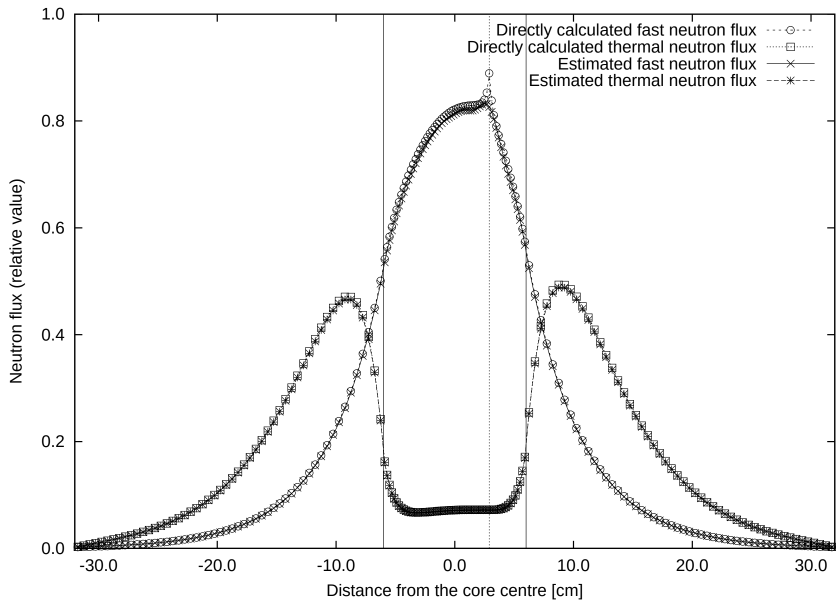

Fig. 3.15 Estimated neutron flux distribution in the successful case of the higher mode source multiplication method.

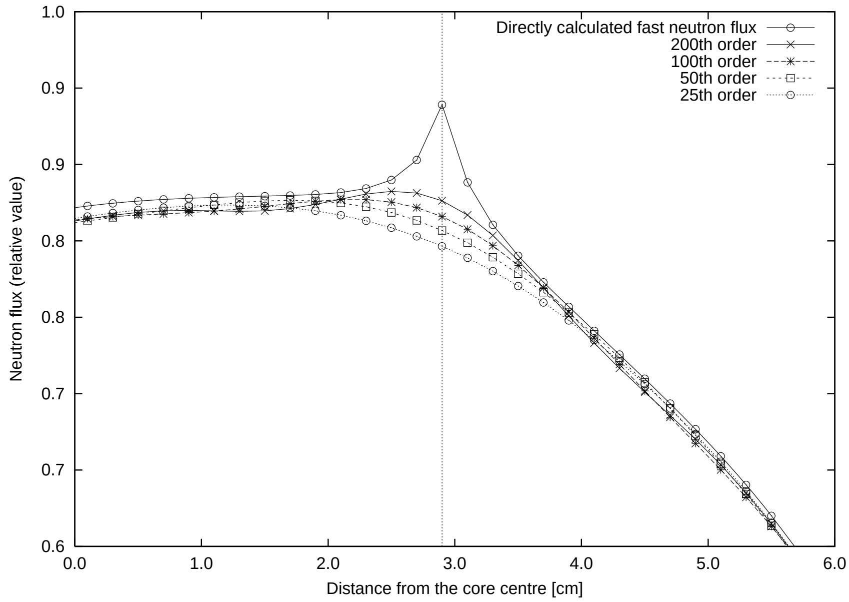

Fig. 3.16 Dependence of the estimated neutron flux distribution on the number of orders taken into account. (dotted line is the position of the external neutron source.)

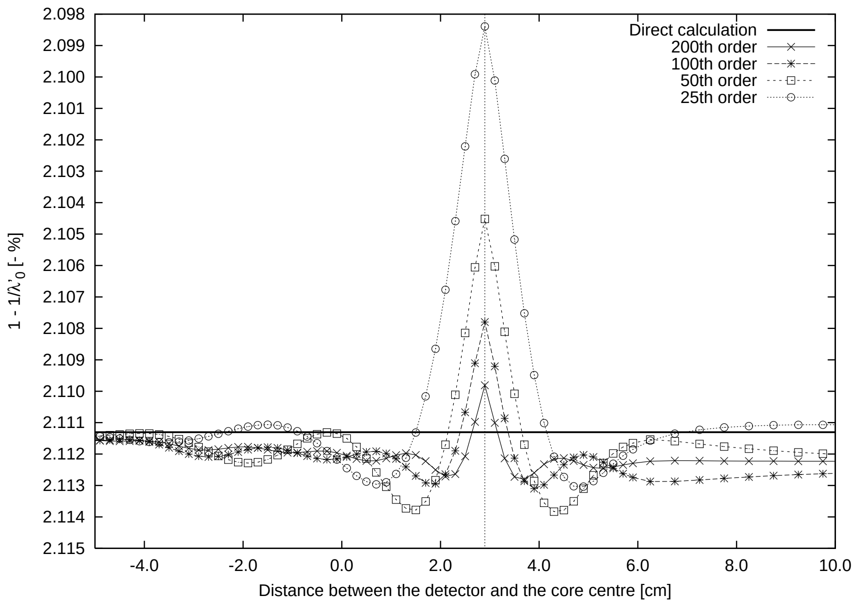

Fig. 3.17 Dependence of the estimated subcriticality on the number of orders of eigenfunctions

following two assumptions are satisfied by chance:

- The neutron flux distribution function in the final state can be expanded with the eigenfunctions of the initial state.
- Operator Σ_Δ can be expressed as $\Sigma_\Delta = RM$, where R is a real number, and M is the creation operator in the initial state.

3.3.2 The Impossible Case of Expansion with the Eigenfunctions

The case that the external neutron source is placed in the reflector region is examined in this section. The subcriticality is changed by the uniform reduction of $\nu\Sigma_f$ by 1 % and the higher mode source multiplication method with the 200th expansion mode was applied as well as the previous case. The core configuration is shown in Fig. 3.18. As is described before, the neutron flux distribution function cannot be expanded with eigenfunctions in this case, and so the higher mode source multiplication method does not work well, as shown in Fig. 3.19. The results by the higher mode source multiplication method are still more accurate than those of the one point reactor approximation, although the error is unacceptably large when the detector is placed nearby the external neutron source represented by the dotted line.

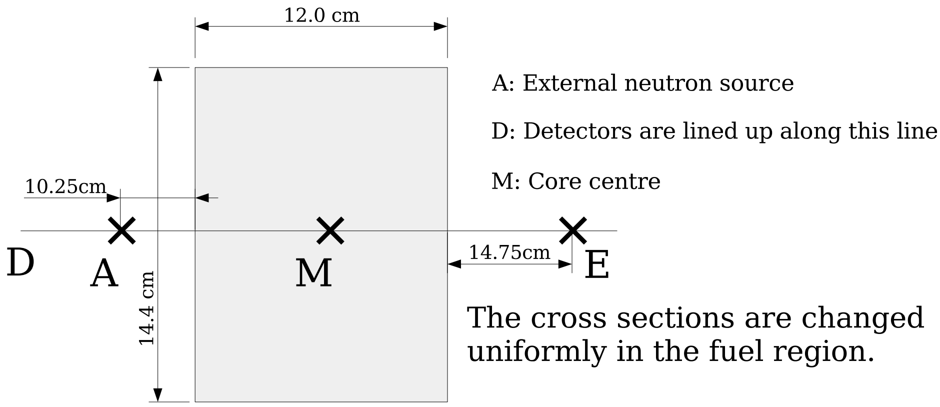

Fig. 3.18 Calculation system for the failing case of the higher mode source multiplication method

This error is caused just because the neutron flux distribution function in the final state cannot be expanded by the eigenfunctions as shown in Figs. 3.20 and 3.21, which show the estimated neutron flux distribution by the neutron detector placed at position E. These figures show a good agreement between the estimated neutron flux distribution and the directly calculated distribution in the reflector region on the right side of the fuel region, while the discrepancy between those two distributions is quite large nearby the external neutron source. This discrepancy is caused by the incompleteness of the eigenfunctions. However, the discrepancy is roughly moderated by the fuel, so that it is not very large in the reflector region on the opposite side. This moderation can be hardly guaranteed by theoretical bases.

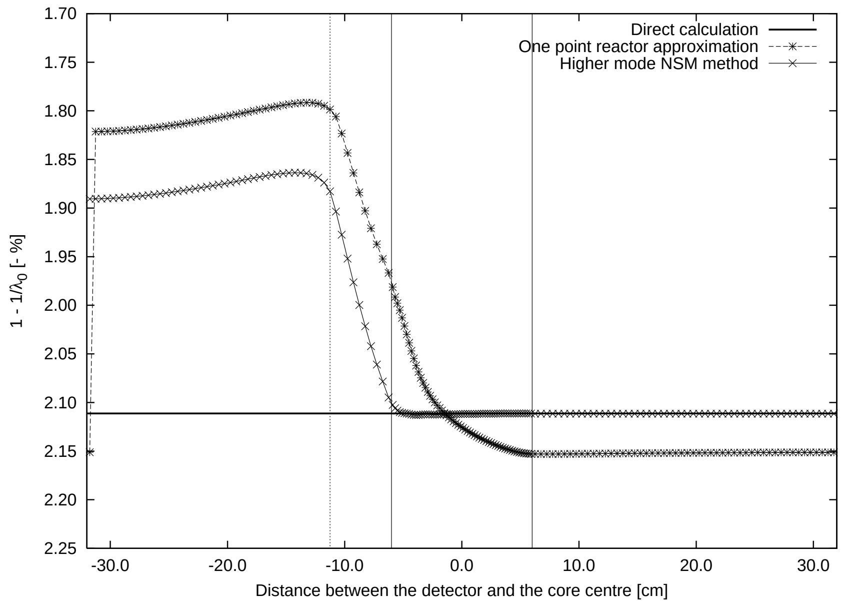

Fig. 3.19 Estimated subcriticality by the higher mode source multiplication method for the external neutron source in the reflector region in comparison with that by the one point reactor approximation. (Solid vertical lines: fuel region, dotted line: the external neutron source.)

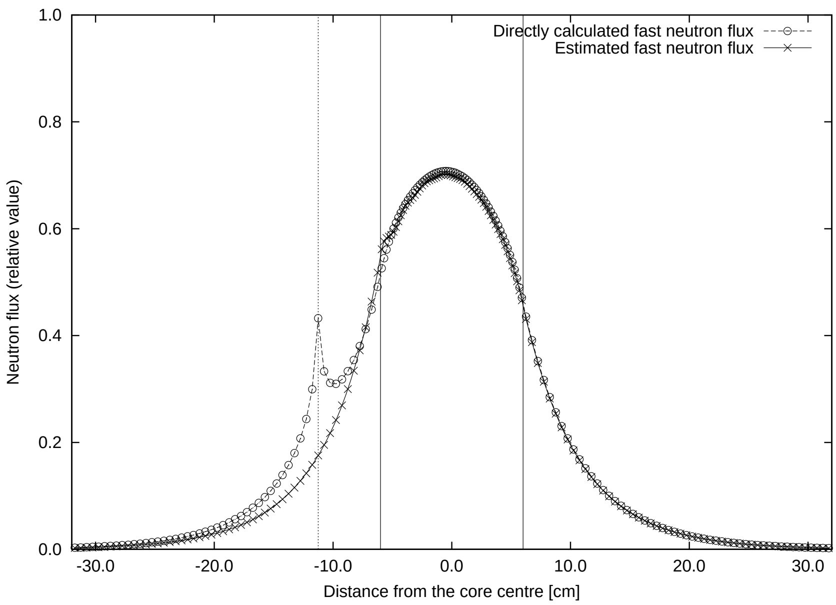

Fig. 3.20 Estimated fast neutron flux distribution by the higher mode source multiplication method for the external neutron source in the reflector region

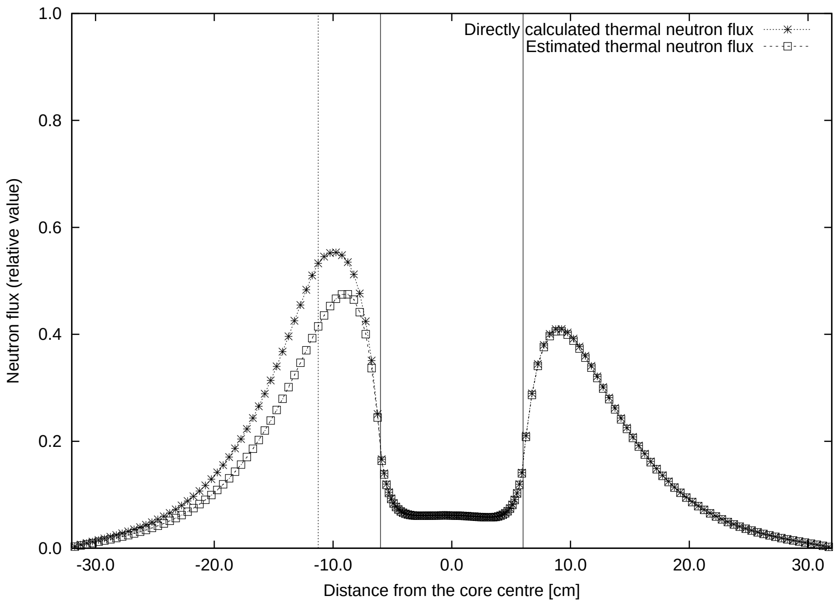

Fig. 3.21 Estimated thermal neutron flux distribution by the higher mode source multiplication method for the external neutron source in the reflector region

In this case, the advantage of the imaginary source multiplication method is explicitly shown. Operator $\Sigma_{\Delta 1}$ can be defined as the following matrix:

$$\Sigma_{\Delta 1} \equiv \begin{pmatrix} -\nu\Sigma_{f1} & -\nu\Sigma_{f2} \\ 0 & 0 \end{pmatrix} \quad . \tag{3.11}$$

Among the results of the 1st order imaginary source multiplication method, almost no dependence on the detector position was observed, as shown in Fig. 3.22. The error was less than $1 \times 10^{-3}\% \frac{\Delta k}{k}$ at most. Almost no dependence on the detector position has been observed, even when the neutron detector was placed nearby the external neutron source.

As a conclusion, when the external neutron source is placed in the reflector region, the measurement results of the higher mode source multiplication method is dependent on the detector position. This dependence comes from the assumption of the completeness of the eigenfunctions. Even if the external neutron source is placed in the reflector region, the results of the imaginary source multiplication method shows almost no dependence on the detector position because the completeness of the eigenfunctions is not assumed in the theory.

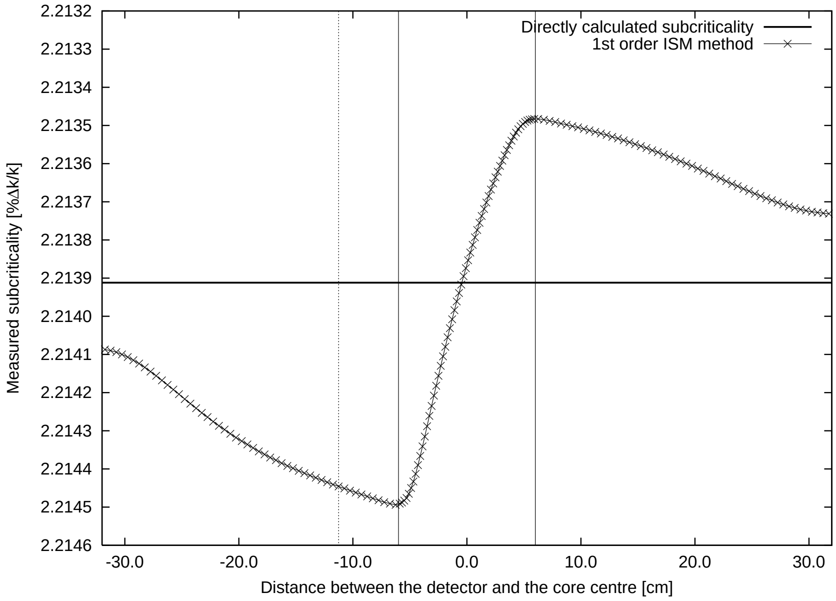

Fig. 3.22 Estimated subcriticality by the imaginary source multiplication.

3.3.3 The Case of the Local Change of Cross Sections

Another example of the disability of the higher mode source multiplication method is demonstrated in this section. The external neutron source is placed at position C shown in Fig. 3.23, and $\nu\Sigma_f$ is reduced by 15 % only in region B. In this case, the reduction of $\nu\Sigma_f$ is represented as an imaginary neutron source with the spectrum of $-a\chi$, where a is a positive constant and χ the fission spectrum. Thus the expansion with eigenfunctions itself is supposed to be possible, but this situation does not satisfy the assumption of Eq. (1.25). The higher mode source multiplication method cannot be applied.

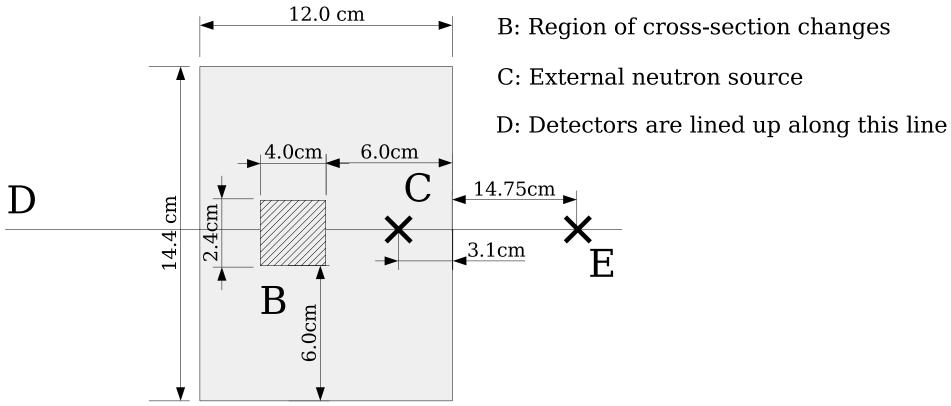

Fig. 3.23 Calculation system for the failing case of the higher mode source multiplication method

Figure 3.24 shows the results of the higher mode source multiplication method with the 200th expansion mode. Region B is represented by the broken lines. In this case, the measurement results are inaccurate regardless of the detector position.

The estimated neutron flux distribution when the neutron detector is placed at position E is shown in Fig. 3.25. In this figure, some discrepancy between the estimated fast neutron flux distribution and the directly calculated one is observed around region B, as shown in Fig. 3.26. This discrepancy, which indicates the failure for the expansion of the neutron flux distribution function with the eigenfunctions, is the origin of the measurement error.

Figure 3.27 shows the measurement results by the 1st order imaginary source multiplication method,

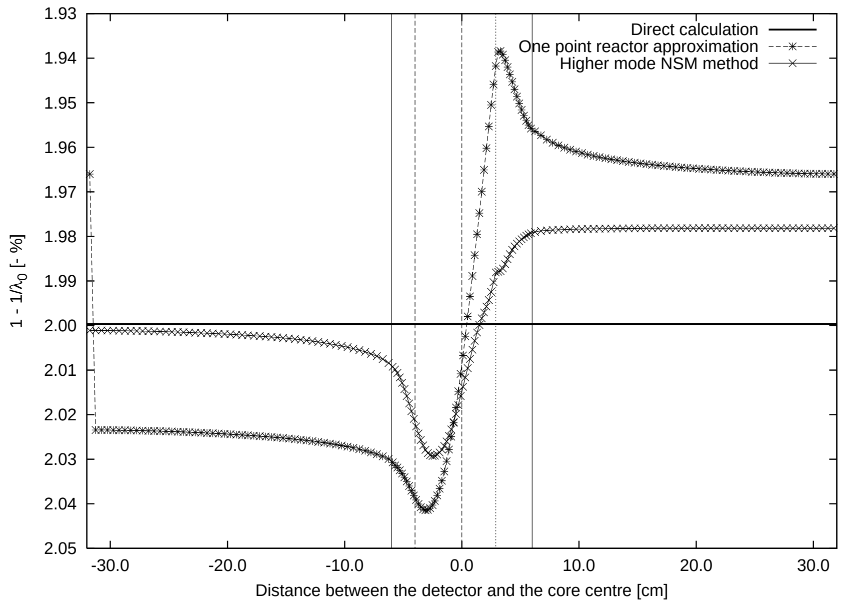

Fig. 3.24 Results of the higher mode source multiplication method for the local change of cross sections. (Solid vertical lines: fuel region, broken: region of cross section change, dotted: the external neutron source.)

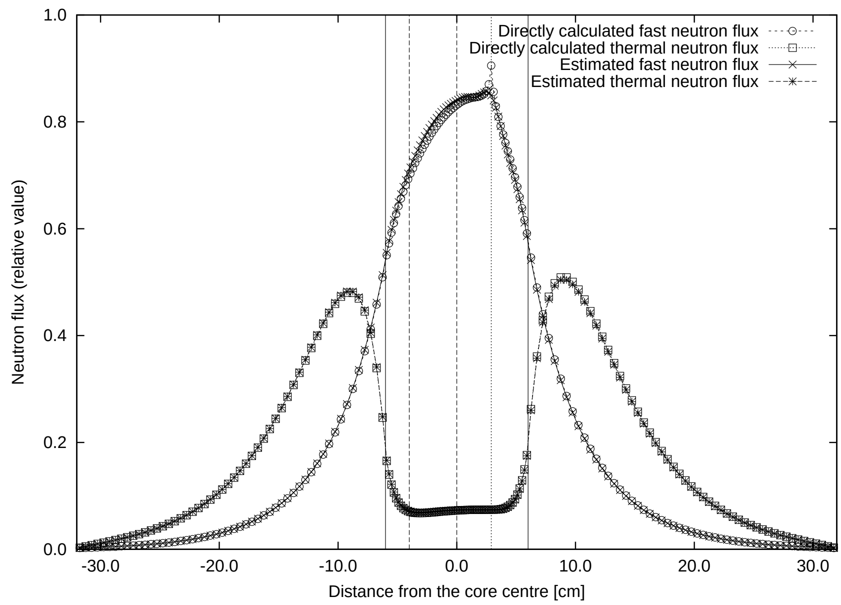

Fig. 3.25 Estimated neutron flux distribution in the case of the local change of cross sections in comparison with the direct calculation.

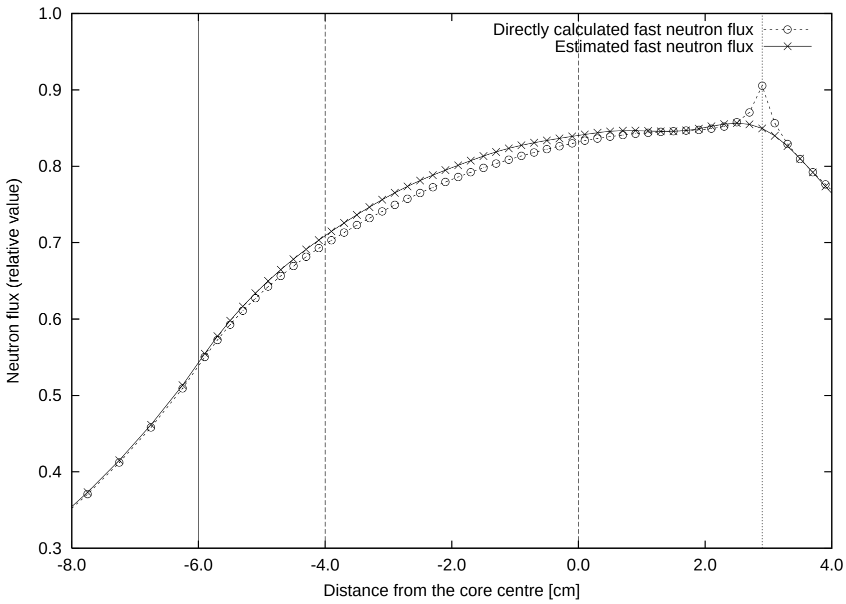

Fig. 3.26 Discrepancy between the estimation by the higher mode source multiplication method and the direct calculation.

where operator $\Sigma_{\Delta 1}$ is defined as

$$\Sigma_{\Delta 1} \equiv \begin{pmatrix} -\nu\Sigma_{f1} & -\nu\Sigma_{f2} \\ 0 & 0 \end{pmatrix} \quad . \tag{3.12}$$

This definition is based on the same assumption with the higher mode source multiplication method, namely Eq. (1.25). In order to compare the results by the imaginary source multiplication method with those by the higher mode source multiplication method, the error between the results of the measurement and the direct calculation is plotted in Fig. 3.28. Both results have similar dependence on the detector position. This dependence comes from the definition of Eq. (3.12), which is inappropriate in this case.

As a conclusion, both the imaginary source multiplication method and the higher mode source multiplication method cannot estimate the subcriticality accurately as long as the inappropriate assumption of Eq. (3.12) is employed. These results indicate that the advantage of the imaginary source multiplication method over the higher mode source multiplication method is just the flexibility of the definition of operators $\Sigma_{\Delta j}$. If operators $\Sigma_{\Delta j}$ are defined inappropriately, the imaginary source multiplication method is as inaccurate as the higher mode source multiplication method.

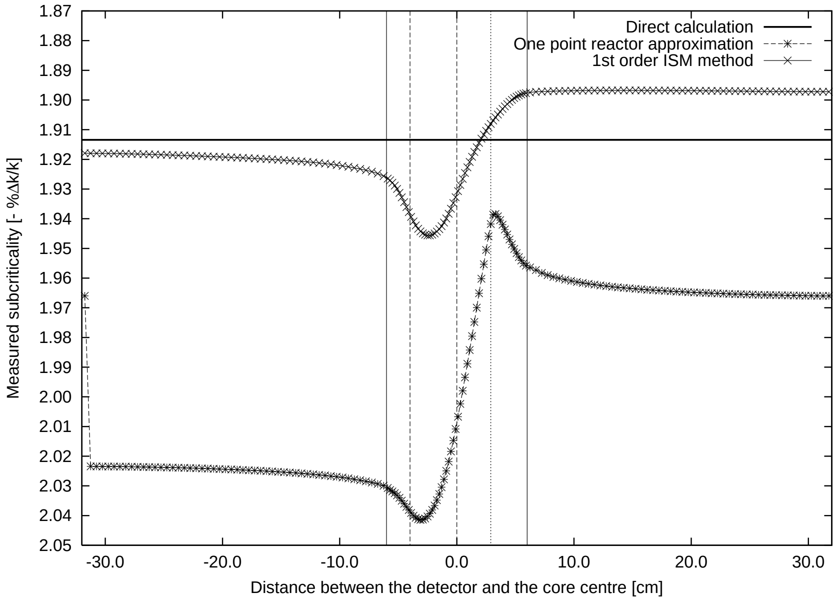

Fig. 3.27 Measurement results by the 1st order imaginary source multiplication method in comparison with those by the one point reactor approximation.

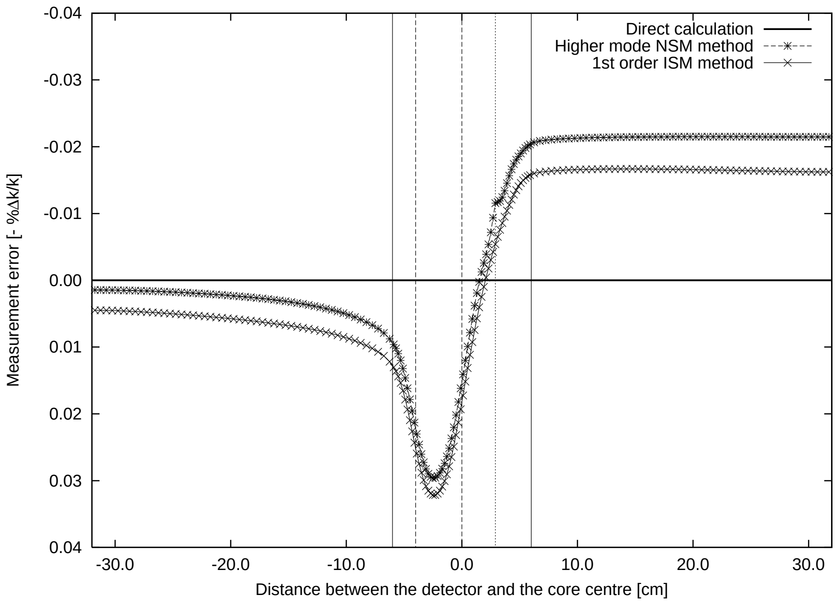

Fig. 3.28 Comparison between the results by two methods, the higher mode source multiplication method and the 1st order imaginary source multiplication method.

3.4 Imaginary Source Multiplication Method with Two Neutron Detectors

In this section, the case of $N = 2$ is numerically investigated. $\nu\Sigma_f$ was reduced uniformly by 0.5 %, and Σ_a and $\nu\Sigma_f$ were additionally reduced in region B by 7.5 % and 15.0 %, respectively. The calculation system is shown in Fig. 3.29.

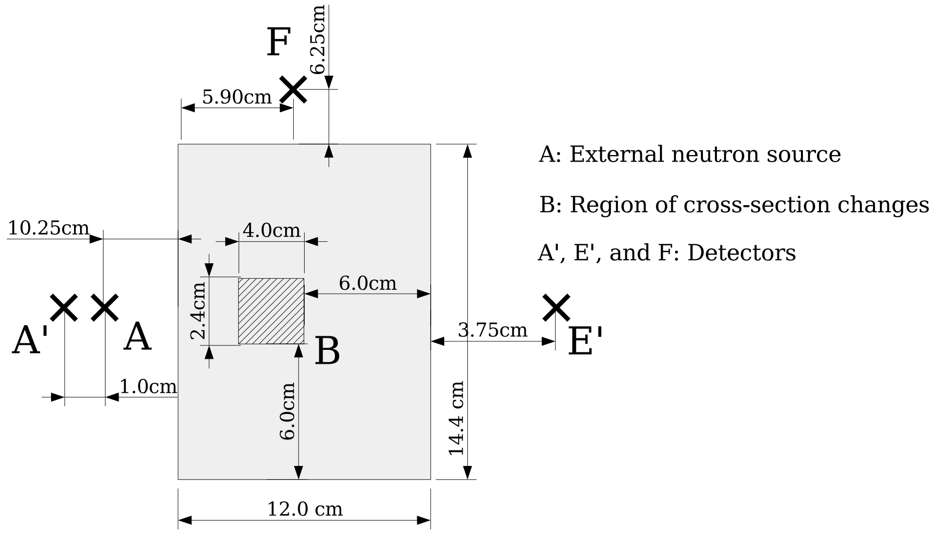

Fig. 3.29 Calculation system for the case of two neutron detectors

Σ_Δ can be represented as

$$\Sigma_\Delta = \begin{cases} \begin{pmatrix} -0.155\nu\Sigma_{f1} + 0.075\Sigma_{a1} & -0.155\nu\Sigma_{f2} \\ 0 & 0.075\Sigma_{a2} \end{pmatrix} & \text{(inside region } B) \\ \begin{pmatrix} -0.005\nu\Sigma_{f1} & -0.005\nu\Sigma_{f2} \\ 0 & 0 \end{pmatrix} & \text{(outside region } B) \end{cases} . \tag{3.13}$$

Known operators $\Sigma_{\Delta 1}$ and Σ_{Δ_2} are chosen as follow:

$$\Sigma_{\Delta 1} \equiv \begin{pmatrix} -\nu\Sigma_{f1} & -\nu\Sigma_{f2} \\ 0 & 0 \end{pmatrix} , \tag{3.14}$$

and

$$\Sigma_{\Delta 2} \equiv \begin{cases} \begin{pmatrix} -\nu\Sigma_{f1} + \frac{1}{2}\Sigma_{a1} & -\nu\Sigma_{f2} \\ 0 & \frac{1}{2}\Sigma_{a2} \end{pmatrix} & \text{(inside region } B\text{)} \\ \begin{pmatrix} 0 & 0 \\ 0 & 0 \end{pmatrix} & \text{(outside region } B\text{)} \end{cases} \quad . \tag{3.15}$$

Coefficients C_j, which are assumed to be unknown, are

$$C_1 = 0.005 \quad \text{and} \quad C_2 = 0.15 \quad . \tag{3.16}$$

The external neutron source is assumed to be placed at position A shown in Fig. 3.29, and neutron detectors are placed at two points out of A', E', and F. The result of the direct calculation of subcriticality was $2.2493\%\frac{\Delta k}{k}$.

Table 3.2 shows the calculation results of i-th order imaginary source multiplication method by using the correction with R_i.

Table 3.2 Calculation results in the case of $N = 2$

Detector position	i	Subcriticality $[\%\frac{\Delta \mathrm{k}}{\mathrm{k}}]$	C_1	C_2	R_i
A' and E'	1	2.2460	5.0640×10^{-3}	1.5692×10^{-1}	5.1618×10^{-1}
	3	2.2464	5.0807×10^{-3}	1.5607×10^{-1}	5.5431×10^{-1}
	5	2.2466	5.0977×10^{-3}	1.5532×10^{-1}	5.9230×10^{-1}
	7	2.2468	5.1134×10^{-3}	1.5462×10^{-1}	6.2980×10^{-1}
E' and F	1	2.2453	5.3952×10^{-3}	1.4679×10^{-1}	5.1621×10^{-1}
	3	2.2456	5.4195×10^{-3}	1.4577×10^{-1}	5.5361×10^{-1}
	5	2.2458	5.4479×10^{-3}	1.4471×10^{-1}	5.9078×10^{-1}
	7	2.2460	5.4743×10^{-3}	1.4372×10^{-1}	6.2737×10^{-1}

The estimated values of subcriticality are quite accurate and they seem convergent on the directly calculated value. By contrast, the estimated values of C_1 and C_2 are dependent on the detector position. This dependence comes from the fact that the values of C_j as the solutions of the simultaneous equations (2.29) are quite sensitive to the values of n_l', while n_l' usually include some errors. Although the estimated values of C_1 and C_2 are not very accurate, these errors do not cause significant errors on the estimation of neutron flux distribution, since the neutron flux distribution is not very sensitive to such small difference of macroscopic cross sections.

As a result, the subcriticality can be estimated in good accuracy, while the estimated amount of the changes of macroscopic cross sections, which are shown as C_j, is slightly dependent on the detector position.

§4 Application to the Experiment in Kyoto University Critical Assembly

4.1 Setup of the Experimental System

In Section 3, the theoretical validity of the imaginary source multiplication method has been confirmed. The results of the imaginary source multiplication method are supposed to be equivalent to those of the direct calculation. However, in the experiment, there are always some errors between the results of the numerical calculation and those of the measurement. This discrepancy appears as a difference between the measured count rates of neutron detectors and the calculated reaction rates of them. This difference is, from another viewpoint, equivalent to the error of calculation in the imaginary neutron source distribution. Therefore, the experimental verifications are required in order to examine the impact of this error in calculation on the results of measurement.

The experimental verifications of the imaginary source multiplication method have been performed at the C-core of Kyoto University Critical Assembly (KUCA)[22,23] in Kyoto University Research Reactor Institute. The C-core is composed of the 93 % highly enriched uranium fuel and the light water as moderator and reflector. The core configuration is shown in Fig. 4.1.

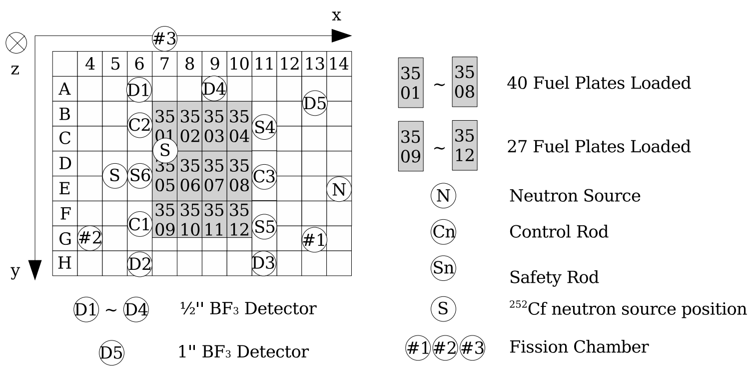

Fig. 4.1 Core configuration employed in the experiment

Throughout the experiment, control rod C3 had been fully inserted to the lower limit, and other control rods, including safety rods, had been fully withdrawn up to the upper limit. When the 428 fuel plates were loaded, the largest eigenvalue, λ_0, which was measured by the rod drop method based on the one point reactor approximation was 0.9949. Then the subcriticality was changed by the substitution of aluminium plates for the fuel plates.

The required numerical calculations were conducted by the 3-dimensional and 107-group diffusion calculation by the SRAC2003 CITATION code with JENDL-3.3. The system was divided into $60 \times 70 \times 70$ grids. In the calculations, the value of ^{235}U density was decreased by 2.2 %, so that the calculated λ_0 for the core loaded with 428 fuel plates becomes to be 0.99487.

For the imaginary source multiplication method, this system loaded with 428 fuel plates was chosen as the calibration system, which is defined in Section 2.2.4. As the initial state, the system loaded with 328 fuel plates was chosen. In order to calculate the macroscopic cross sections of the initial state, the thickness of fuel meat of each fuel plate was assumed to be reduced to $\frac{328}{428}$ of the real value, while the whole thickness of fuel plates was conserved.

4.2 Results of the Experiment

Table 4.1 shows the measured subcriticality with the imaginary source multiplication method by using the correction with R_i where fuel plates were uniformly substituted in all frames. The position of the substituted plates were chosen so that the aluminium plates were placed with constant distance between one another. The ^{252}Cf external neutron source was placed at the position of (C-D, 7) shown in Fig. 4.1. The number of required detectors, denoted by N, was unity. Operator $\Sigma_{\Delta 1}$ was defined as a 107×107 matrix which has the following (i, j) components, denoted by $(\Sigma_{\Delta 1})_{ij}$:

$$(\Sigma_{\Delta 1})_{ij} \equiv \delta_{i,j} \left(\nabla \Delta D_i \nabla - \Delta \Sigma_{ti} \right) + \chi_j \nu \Delta \Sigma_{fi} + \Delta \Sigma_{s\ i \to j} \quad , \tag{4.1}$$

where $\delta_{i,j}$ is Kronecker delta. ΔD_i, $\Delta \Sigma_{fi}$, and $\Delta \Sigma_{ti}$ represent the calculated difference in diffusion coefficient, fission cross section, and total cross section of the i-th group, respectively, between the initial state and the system that all the fuel plates were substituted with aluminium plates. $\Delta \Sigma_{s\ i \to j}$ is the difference in scattering cross section from the i-th group to the j-th group, between these two systems, and the fission spectrum is denoted by χ_j. The neutron flux at a certain point is expressed as a vertical vector.

In Table 4.1, the columns of '1st order' and '3rd order' show the measurement results by using the 1st and 3rd order imaginary source multiplication methods, respectively. The correction with R_i was applied. The columns of 'One point' represent the results by using the ordinary neutron source multiplication method with the one point reactor approximation. The rows of 'Std. Dev.' show the standard deviation among the results by each detector. The standard deviation indicates the magnitude of dependence on the detector positions. The rows of 'Direct calc.' show the results of the direct calculation by CITATION. For these direct calculations, the thickness of fuel meat of each fuel plate was adjusted so that the ratio of the count rates of neutron detector D5 between the initial state and the final state agrees with that of the calculated reaction rates.

The measurement results by the 3rd order imaginary source multiplication method have agreed with those of the direct calculations when 386 and 358 fuel plates were loaded. Almost no dependence on the detector position was observed. By contrast, in the cases that 322 and 288 fuel plates were loaded, the results of the imaginary source multiplication method show larger standard deviation than those of the

Table 4.1 Results of subcriticality measurement (source in the fuel region)

	386 loaded fuel plates			358 loaded fuel plates		
	Estimated subcriticality $\left[-\%\frac{\Delta k}{k}\right]$					
Detector	1st order	3rd order	One point	1st order	3rd order	One point
D1	2.57 ± 0.08	2.86 ± 0.07	3.19 ± 0.07	4.74 ± 0.16	4.78 ± 0.15	4.96 ± 0.13
D2	2.46 ± 0.10	2.79 ± 0.08	2.69 ± 0.08	4.39 ± 0.16	4.46 ± 0.15	4.37 ± 0.16
D3	2.40 ± 0.13	2.75 ± 0.11	2.55 ± 0.10	4.39 ± 0.16	4.46 ± 0.14	4.30 ± 0.15
D4	2.53 ± 0.05	2.84 ± 0.04	2.94 ± 0.04	4.65 ± 0.10	4.70 ± 0.09	4.75 ± 0.09
D5	2.42 ± 0.06	2.76 ± 0.05	2.66 ± 0.05	4.38 ± 0.11	4.45 ± 0.10	4.36 ± 0.11
Std Dev.	0.06	0.04	0.23	0.16	0.14	0.26
Direct calc.	2.76			4.46		

	322 loaded fuel plates			288 loaded fuel plates		
Detector	1st order	3rd order	One point	1st order	3rd order	One point
D1	7.84 ± 0.28	7.94 ± 0.31	7.50 ± 0.23	11.25 ± 0.27	11.77 ± 0.30	10.32 ± 0.22
D2	6.73 ± 0.32	6.75 ± 0.30	6.83 ± 0.37	9.32 ± 0.30	9.66 ± 0.34	10.29 ± 0.45
D3	7.16 ± 0.23	7.21 ± 0.25	7.46 ± 0.30	9.58 ± 0.28	9.99 ± 0.33	11.28 ± 0.52
D4	7.41 ± 0.18	7.48 ± 0.19	7.39 ± 0.18	10.34 ± 0.22	10.79 ± 0.25	10.63 ± 0.26
D5	7.07 ± 0.13	7.11 ± 0.14	7.23 ± 0.16	9.78 ± 0.17	10.18 ± 0.19	11.00 ± 0.27
Std Dev.	0.37	0.40	0.24	0.69	0.74	0.39
Direct calc.	7.13			10.31		

ordinary neutron source multiplication method with the one point reactor approximation. This error comes from the fact that the accuracy of the numerical calculation becomes poorer as the subcriticality becomes larger.

Table 4.2 shows the results of estimation for the change of macroscopic cross sections. No significant dependence on the detector position was observed except for detector D1, and all the obtained values were underestimated.

Table 4.2 Estimated number of loaded fuel plates (source in fuel region)

	Number of loaded fuel plates							
	386		358		322		288	
	Estimated number of loaded fuel plates							
Detector	1st	3rd	1st	3rd	1st	3rd	1st	3rd
D1	375 ± 2	377 ± 1	344 ± 3	345 ± 2	302 ± 3	302 ± 4	258 ± 2	259 ± 2
D2	377 ± 3	377 ± 1	350 ± 3	350 ± 3	317 ± 4	317 ± 4	282 ± 3	283 ± 3
D3	378 ± 4	379 ± 2	350 ± 3	350 ± 2	311 ± 3	311 ± 3	279 ± 2	279 ± 3
D4	376 ± 1	377 ± 1	346 ± 2	346 ± 1	308 ± 2	308 ± 2	269 ± 2	270 ± 2
D5	378 ± 2	379 ± 1	350 ± 2	350 ± 2	312 ± 2	312 ± 2	277 ± 2	277 ± 2

These errors were merely caused by the lack of accuracy in the numerical calculation. In particular, the ratio of the measured count rates by the detector between the calibration system and the final state did not agree with that of the calculated reaction rates in the detector between the two states. The impact of this disagreement is discussed in Section 4.3.

Tables 4.3 and 4.4 show the measured results when the ^{252}Cf external neutron source was placed at position (D-E, 5) shown in Fig. 4.1. As same as the case that the external neutron source was placed in the fuel region, the obtained results by the imaginary source multiplication method are not accurate when the subcriticality is large. In particular, the results obtained by neutron detectors D1 and D2 are inaccurate. The origin of these errors is that the accuracy of the calculated neutron flux around the external neutron source is relatively poor compared with other positions.

As a conclusion, the results of measurement by the imaginary source multiplication method is accurate

Table 4.3 Results of subcriticality measurement (source in the reflector region)

	386 loaded fuel plates			358 loaded fuel plates		
	Estimated subcriticality $\left[-\%\frac{\Delta k}{k}\right]$					
Detector	1st order	3rd order	One point	1st order	3rd order	One point
D1	3.08 ± 0.17	3.39 ± 0.15	3.63 ± 0.14	5.29 ± 0.30	5.34 ± 0.28	5.48 ± 0.26
D2	3.42 ± 0.27	3.66 ± 0.24	4.17 ± 0.22	6.07 ± 0.43	6.08 ± 0.42	6.23 ± 0.33
D3	2.81 ± 0.19	3.17 ± 0.16	2.95 ± 0.15	4.95 ± 0.27	5.04 ± 0.25	4.86 ± 0.26
D4	2.93 ± 0.13	3.27 ± 0.11	3.12 ± 0.10	5.12 ± 0.20	5.19 ± 0.19	5.07 ± 0.20
D5	2.88 ± 0.14	3.24 ± 0.11	2.95 ± 0.11	4.93 ± 0.18	5.01 ± 0.16	4.78 ± 0.17
Std Dev.	0.22	0.17	0.47	0.42	0.39	0.53
Direct calc.	2.76			4.46		

	322 loaded fuel plates			288 loaded fuel plates		
Detector	1st order	3rd order	One point	1st order	3rd order	One point
D1	8.58 ± 0.35	8.67 ± 0.38	8.39 ± 0.32	12.30 ± 0.64	12.87 ± 0.73	11.93 ± 0.63
D2	10.04 ± 0.82	10.27 ± 0.91	9.12 ± 0.57	14.98 ± 1.05	15.77 ± 1.15	12.43 ± 0.67
D3	8.04 ± 0.34	8.09 ± 0.37	8.36 ± 0.46	11.05 ± 0.44	11.52 ± 0.51	13.13 ± 0.83
D4	7.88 ± 0.97	7.92 ± 1.04	8.09 ± 1.21	11.31 ± 0.33	11.80 ± 0.38	13.11 ± 0.57
D5	7.90 ± 0.20	7.95 ± 0.22	8.26 ± 0.28	10.88 ± 0.28	11.34 ± 0.32	13.28 ± 0.57
Std Dev.	0.81	0.89	0.35	1.52	1.64	0.52
Direct calc.	7.13			10.31		

Table 4.4 Estimated number of loaded fuel plates (source in reflector region)

	Number of loaded fuel plates							
	386		358		322		288	
	Estimated number of loaded fuel plates							
Detector	1st	3rd	1st	3rd	1st	3rd	1st	3rd
D1	365 ± 3	367 ± 2	342 ± 4	342 ± 3	309 ± 3	310 ± 3	274 ± 4	275 ± 3
D2	362 ± 5	362 ± 3	334 ± 5	334 ± 4	295 ± 6	296 ± 6	250 ± 5	252 ± 3
D3	368 ± 4	368 ± 2	345 ± 3	345 ± 3	315 ± 3	315 ± 3	286 ± 3	286 ± 3
D4	367 ± 2	367 ± 2	344 ± 3	344 ± 2	316 ± 8	316 ± 9	283 ± 2	284 ± 2
D5	367 ± 3	368 ± 2	346 ± 2	346 ± 2	316 ± 2	316 ± 2	287 ± 2	287 ± 2

only when the numerical calculation can provide the result accurately. If the numerical calculation were suffered from large error, the results of the measurement might become less accurate than the ordinary neutron source multiplication method with the one point reactor approximation.

4.3 Analyses of the Impact of Calculation Accuracy

The observed errors in the experiment are merely caused by the lack of accuracy of numerical calculations. For the confirmation of this fact, Tables 4.5 and 4.6 show the measurement results where the ratio of the calculated reaction rates is used instead of that of the measured count rates. This is equivalent to the assumption that the numerical calculation includes no errors. These results of the imaginary source multiplication method show good accuracy. Almost no dependence on the detector position has been observed. As a result, the errors in the experiment are considered to be merely caused by the inaccurate numerical calculation.

In order to obtain accurate results, the position of the neutron detector should be chosen so that the estimated value of the subcriticality is not sensitive to the calculation error. The sensitivity has been numerically investigated. Figures 4.2 through 4.5 show the dependence of the measurement results on the accuracy of calculation. The vertical axis represents the estimated subcriticality by the imaginary source multiplication method with the correction of R_i when the count rates of the neutron detector in the initial state and the final state were $n_{0,\mathrm{ex}}$ and n'_{ex}, respectively. The horizontal axis is the value of

$$\left(1 - \frac{n'_{\mathrm{ex}}}{n_{0,\mathrm{ex}}}\right)\left(1 - \frac{n'_{\mathrm{calc}}}{n_{0,\mathrm{calc}}}\right)^{-1} - 1 \quad , \tag{4.2}$$

where $n_{0,\mathrm{calc}}$ and n'_{calc} are the calculated reaction rate of the neutron detector in the initial state and the final state, respectively. The value of expression (4.2) represents the error between the experiment and the calculation. For instance, 10% of this value corresponds to the case that the calculation overestimates the change of reaction rate by 9 % compared with that of the experimental count rates.

These figures show approximately linear relations between the estimated subcriticality and the value of expression (4.2). Almost no difference has been observed among the curves obtained at each detector position. The sensitivity of the estimated subcriticality to the calculation accuracy is represented as the gradient of the plotted curve, which is almost independent of the detector position. In other words, the tolerability of the results of the imaginary source multiplication method to the calculation error does not depend on the detector position.

Therefore, in order to reduce the measurement error, the neutron detectors should be placed where the precision of the numerical calculation of the neutron flux is relatively high, without caring the impact

Table 4.5 Results obtained by using the calculated reaction rates. (source in the fuel region, corresponding to Table 4.1)

	386 loaded fuel plates			358 loaded fuel plates		
	Estimated subcriticality $\left[-\%\frac{\Delta k}{k}\right]$					
Detector	1st order	3rd order	One point	1st order	3rd order	One point
D1	2.41	2.73	3.07	4.39	4.46	4.67
D2	2.39	2.73	2.63	4.31	4.39	4.29
D3	2.38	2.73	2.53	4.24	4.33	4.16
D4	2.40	2.73	2.83	4.39	4.46	4.51
D5	2.39	2.73	2.64	4.39	4.46	4.37
Std Dev.	0.01	< 0.01	0.19	0.06	0.05	0.18
Direct calc.	2.76			4.46		

	322 loaded fuel plates			288 loaded fuel plates		
Detector	1st order	3rd order	One point	1st order	3rd order	One point
D1	7.10	7.14	6.89	9.86	10.21	9.16
D2	7.09	7.14	7.26	9.75	10.16	10.95
D3	7.09	7.13	7.36	9.72	10.15	11.53
D4	7.10	7.14	7.07	9.82	10.19	10.02
D5	7.09	7.13	7.26	9.76	10.16	10.97
Std Dev.	0.01	< 0.01	0.17	0.05	0.02	0.84
Direct calc.	7.13			10.31		

Table 4.6 Results obtained by using the calculated reaction rates. (source in reflector region, corresponding to Table 4.3)

	386 loaded fuel plates			358 loaded fuel plates		
	Estimated subcriticality $\left[-\%\frac{\Delta k}{k}\right]$					
Detector	1st order	3rd order	One point	1st order	3rd order	One point
D1	2.72	3.08	3.33	4.96	5.03	5.20
D2	2.74	3.09	3.62	4.96	5.03	5.38
D3	2.71	3.09	2.87	4.96	5.04	4.86
D4	2.71	3.08	2.94	4.95	5.03	4.91
D5	2.70	3.09	2.80	4.95	5.04	4.80
Std Dev.	0.02	< 0.01	0.31	< 0.01	< 0.01	0.22
Direct calc.	3.12			5.05		

	322 loaded fuel plates			288 loaded fuel plates		
Detector	1st order	3rd order	One point	1st order	3rd order	One point
D1	8.01	8.05	7.87	11.08	11.49	10.74
D2	8.01	8.05	7.67	11.13	11.50	9.88
D3	8.00	8.05	8.31	10.98	11.44	13.00
D4	8.00	8.05	8.24	11.02	11.47	12.61
D5	8.00	8.05	8.38	10.95	11.43	13.44
Std Dev.	0.01	< 0.01	0.28	0.07	0.03	1.38
Direct calc.	8.05			11.60		

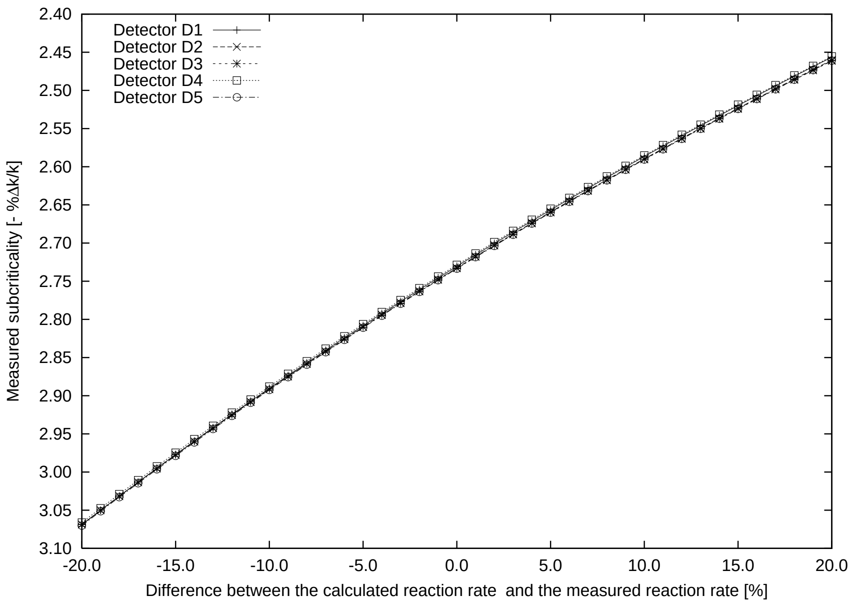

Fig. 4.2 Sensitivity to the calculation accuracy (source in the fuel region, 386 loaded fuel plates)

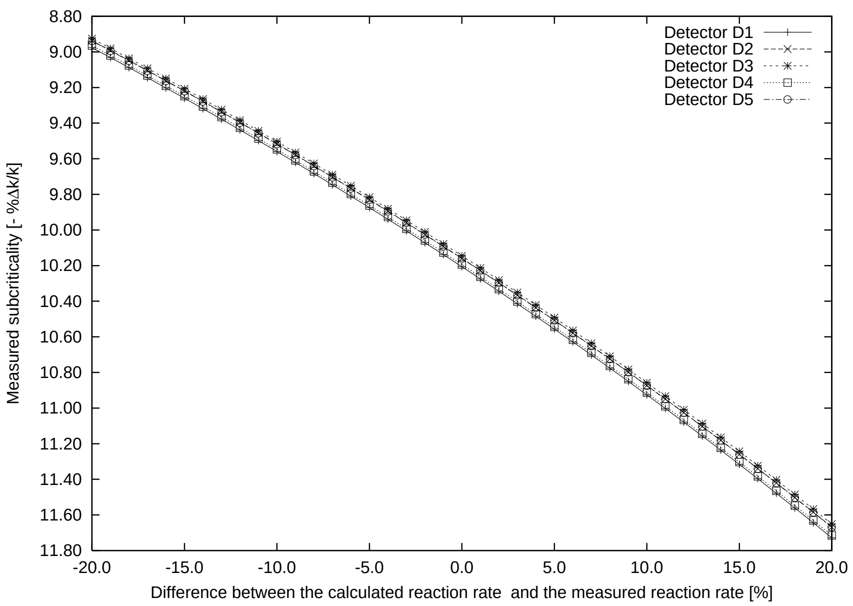

Fig. 4.3 Sensitivity to the calculation accuracy (source in the fuel region, 288 loaded fuel plates)

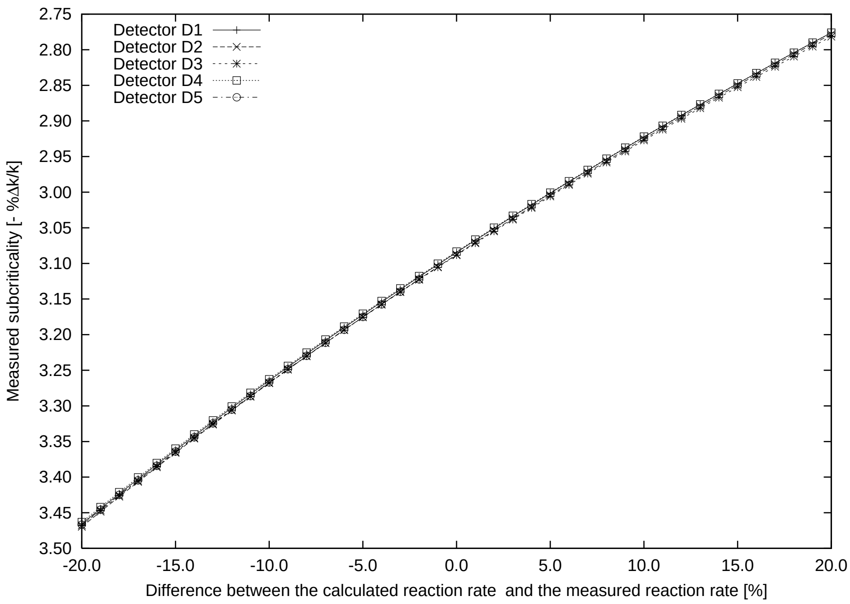

Fig. 4.4 Sensitivity to the calculation accuracy (source in the reflector region, 386 loaded fuel plates)

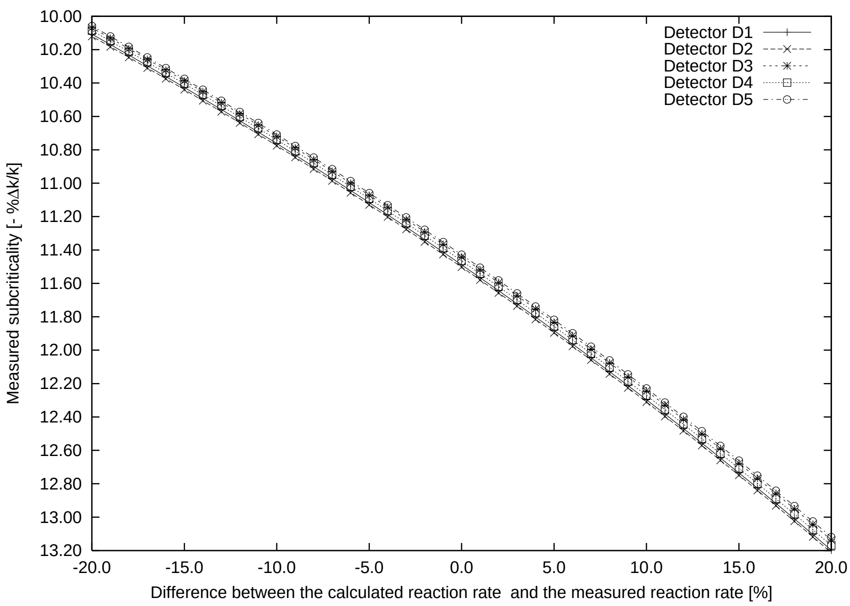

Fig. 4.5 Sensitivity to the calculation accuracy (source in the reflector region, 288 loaded fuel plates)

of the dependence of the sensitivity on the detector position. For instance, the region nearby the external neutron source should be avoided.

§5 Conclusions

Summary

In this paper, the imaginary neutron source multiplication method has been proposed and verified.

The theory of the imaginary source multiplication method has been discussed in Section 2. This new method is aiming to be applied to various systems without losing its theoretical consistency. The essence of this method is to consider the changes of creation and annihilation operators of neutrons as the placement of imaginary neutron sources. The intensity of this imaginary neutron source can be estimated by the combination of the numerical calculation for the initial state and the cont rates of neutron detectors in the final state. This method is based on an assumption that operator Σ_Δ can be expressed as

$$\Sigma_\Delta = \sum_{j=1}^{N} C_j \Sigma_{\Delta j} \quad ,$$

which is Eq. (2.7). Known operators $\Sigma_{\Delta j}$ are arbitrarily chosen so that this assumption is equivalent to our knowledge of the measured system. This method is equivalent to the direct calculation of the measured system whose geometry is not exactly known.

The validity of the imaginary source multiplication method has been demonstrated in Section 3. The measurement results by this method are accurate because no inappropriate assumptions are employed in the theory. Almost no dependence of the measurement result on the detector position had been observed so far as the restriction condition of Eq. (2.7), which is shown above, is satisfied.

However, in the experiment, the estimated subcriticality by the imaginary source multiplication method has not agreed with the directly calculated value, as discussed in Section 4. These errors were caused merely by the lack of accuracy in the numerical calculations. Therefore, in order to obtain accurate results of measurement, the accuracy of the numerical calculation must be improved.

Future works

There are four problems that should be solved.

At first, in the theory of the imaginary source multiplication method, the transformation of Eq. (2.40) to Eq. (2.42) is not mathematically consistent, although it is considered necessary. The validity of this transformation is required to be proved.

Secondly, the imaginary source multiplication method places complete trust in the results of the numerical calculation, but there always exist some differences between the experiment and the calculation. The theory should be modified to assume the existence of these differences, for increasing the tolerance against the calculation errors.

Thirdly, in order to increase the measurement accuracy in the experiment, the calculation method for the imaginary neutron source distribution function is required to be modified. In this paper, the calculation was based on the diffusion calculation. The transport calculation, such as Monte Carlo method, should be introduced.

Finally, the restriction condition of Eq. (2.7) cannot be satisfied in the general cases, including the burnup and the case that the amount of liquid fuel is changing in a container. The formulation of the restriction condition should be generalized.

From the viewpoint of the application to ADS, the latter two problems are especially important. In ADS, the diffusion approximation is inappropriate because the vacuum beam duct exists in the system. Furthermore, complicated changes of the operators are invoked, due to the transmutation and burnup. These phenomena should be expressed in the generalized restriction conditions of operator Σ_{Δ}.

Appendix A Definition of Neutron Flux

In this paper, the discussions are based on the concept of neutron flux. The exact definition of neutron flux should be examined in order to guarantee the rigidness of the theory.

Neutron flux $\phi(\boldsymbol{x}, E)$ is usually defined as

$$\phi(\boldsymbol{x}, E) \equiv v(E) n(\boldsymbol{x}, E) \quad , \tag{A.1}$$

where $v(E)$ is the velocity of neutrons which have kinetic energy E, and $n(\boldsymbol{x}, E)$ the neutron density. The definition of neutron density is ambiguous. If we define neutron density by common sense ignoring the uncertainty principle, it should be like the Dirac delta because the neutron is a particle. Needless to say, this is very inconvenient since the neutron flux distribution functions are implicitly assumed to have finite values.

One candidate of the definition of neutron density is using the time average of the number of neutrons. This definition can be employed if the system is in the so-called steady state. However, steady state is usually defined as a state that neutron density function is time-independent, while the neutron density is not defined yet. This definition is inappropriate here. The steady state can be defined as follows instead: 'if the time-dependent neutron density $n_t(\boldsymbol{x}, E, t)$ is regarded as a probability variable and the probability density function of n_t is independent of time, this state is steady.' Based on this definition of the steady state, neutron density in the steady state can be defined as

$$n(\boldsymbol{x}, E) \equiv \lim_{T \to \infty} \frac{1}{T} \int_0^T n_t(\boldsymbol{x}, E, t) \ \mathrm{d}t \quad , \tag{A.2}$$

which is closely related with the expected value of the probability variable.

The behaviour of neutrons is not purely based on probability, but partially chaotic phenomenon. For instance in a vacuum space, the position of neutron is exactly determined if the initial position and momentum are given. We usually do not know the exact initial state, thus we treat this phenomenon under a certain probability model. Once the probability model has been given, the time-dependent neutron density can be defined as a probability variable. The most important point is that this probability density is not given by the nature, but defined by ourselves just for the convenience.

In the steady state, fortunately, we do not need to give an exact probability model. By just assuming the existence of the probability density function, neutron density can be defined by Eq. (A.2). By contrast, when we extend the discussion to the transitional state, we should be careful of the point that the definition of neutron flux is not given by the nature, but is dependent on the probability model which we employ.

Appendix B Incompleteness of Eigenfunctions

The incompleteness of eigenfunctions plays an important role in the discussion of the subcriticality measurement methods, since some methods are based on the assumption of the completeness. A proof of the incompleteness is shown in this section.

Eigenvalues λ_i and eigenfunctions φ_i are defined as the values and the functions which satisfy the following equation, respectively:

$$L\varphi_i = \frac{1}{\lambda_i} M\varphi_i \quad . \tag{B.1}$$

For the convenience, λ_i are sorted in descending order, then φ_0 is called *fundamental mode* while other φ_i are called *i-th mode* or generally *higher mode.*

When there is an external neutron source which emits neutrons with energy of 1 GeV, the neutron flux distribution cannot be expanded with eigenfunctions because the values of the eigenfunctions are zero at 1 GeV. This is an explicit evidence of incompleteness of eigenfunctions.

Someone still considers that eigenfunctions may be approximated as if complete. Another irrefutable proof is required. Under the diffusion approximation, the equations of the neutron equilibrium at position $\boldsymbol{x}_0$ in the reflector region where an external neutron source exists are

$$-\nabla D \nabla \varphi_i(\boldsymbol{x}_0, E) + \Sigma_t \varphi_i(\boldsymbol{x}_0, E) - \int \Sigma_{s,E' \to E}(\boldsymbol{x}_0, E, E') \varphi_i(\boldsymbol{x}_0, E')\ \mathrm{d}E' = 0 \quad , \tag{B.2}$$

and

$$-\nabla D \nabla \phi(\boldsymbol{x}_0, E) + \Sigma_t \phi(\boldsymbol{x}_0, E) - \int \Sigma_{s,E' \to E}(\boldsymbol{x}_0, E, E') \phi(\boldsymbol{x}_0, E')\ \mathrm{d}E' = S(\boldsymbol{x}_0, E) \quad , \tag{B.3}$$

where ϕ represents the neutron flux distribution function, D the diffusion coefficient, Σ_t the macroscopic total cross section, and S the external neutron source distribution function. When E is enough large that $\Sigma_{s,E' \to E}(\boldsymbol{x}_0, E, E') \approx 0$, from Eq. (B.2),

$$\nabla D \nabla \varphi_i(\boldsymbol{x}_0, E) > 0 \quad , \tag{B.4}$$

for all i. By contrast, when Σ_t is enough small that $S(\boldsymbol{x}_0, E) > \Sigma_t \phi(\boldsymbol{x}_0, E)$, from Eq. (B.3),

$$\nabla D \nabla \phi(\boldsymbol{x}_0, E) < 0 \quad . \tag{B.5}$$

In this case, ϕ cannot be expanded with φ_i around position $\boldsymbol{x}_0$. Therefore, eigenfunctions cannot be generally approximated as if complete.

Finding out necessary, but not sufficient, conditions to approximate the eigenfunctions to be complete is valuable. One of the conditions is, obviously, the external neutron source is in the fuel region. The proof has been already shown above. Another necessary condition is the external neutron source have a certain spectrum, which is supposed to be similar with fission spectrum χ. The proof is shown below.

The reductio ad absurdum (proof by contradiction) is used. The following expansion is assumed to be possible in a steady subcritical system with an arbitrary external neutron source function S:

$$\Psi S = \sum_{i=0}^{\infty} C_i \varphi_i \quad , \tag{B.6}$$

where C_i are the expansion coefficients of i-th mode. These coefficients are dependent on S. Under the G-group approximation, φ_i satisfies the following equation:

$$L\varphi_i = \frac{1}{\lambda_i} M \varphi_i \quad , \tag{B.7}$$

where M and L are $G \times G$ creation and annihilation matrices of neutrons, φ_i the G-dimensional vectors, and λ_i the eigenvalues. φ_i are assumed to be normalized. At the beginning, the number of parameters in Eq. (B.7) is $(G+1)$, namely G dimensions and λ_i. On the other hand, the number of the restriction conditions is G, which is the number of dimensions. The reason why the infinite number of eigenvalues exist is that the number of parameters is larger than that of the restriction conditions. If the values of φ_i at a certain group is given, the number of parameters is reduced to G, and so both φ_i and λ_i are fixed because the number of parameter is no longer larger than that of the restriction conditions. Therefore, in the equation of continuous energy, C_i can be determined by the following equation:

$$\Psi S(\boldsymbol{x}, E_0) = \sum_{i=0}^{\infty} C_i \varphi_i(\boldsymbol{x}, E_0) \quad , \tag{B.8}$$

where E_0 is an arbitrarily chosen energy. This is derived from the fact that no coefficients D_j can satisfy the following relation:

$$\varphi_i(\boldsymbol{x}, E_0) = \sum_{j \neq i} D_j \varphi_j(\boldsymbol{x}, E_0) \quad . \tag{B.9}$$

Another external neutron source distribution function S' can satisfy the following equation:

$$\Psi S'(\boldsymbol{x}, E_0) = \sum_{i=0}^{\infty} C_i \varphi_i(\boldsymbol{x}, E_0) \quad . \tag{B.10}$$

For instance, when S represents a thermal neutron source and E_0 is large enough, S' can be defined as follows:

$$S' = \frac{1}{2}S + \frac{1}{2}M\Psi_{0,L}S \tag{B.11}$$

so that

$$\Psi S' = \Psi S - \frac{1}{2}\Psi_{0,L}S \quad , \tag{B.12}$$

since

$$\Psi S = \Psi_{0,L}S + \Psi M \Psi_{0,L}S \quad . \tag{B.13}$$

The 1st term of the right-hand side in Eq. (B.13) represents the neutrons emitted from the external neutron source, while the 2nd term of that corresponds to the neutrons generated by the fission reaction. By ignoring up-scattering,

$$\Psi_{0,L}S(\boldsymbol{x}, E_0) \approx 0 \quad , \tag{B.14}$$

and so Eq. (B.10) is satisfied.

The contradiction is shown below:

$$\Psi S = \sum_{i=0}^{\infty} C_i \varphi_i = \Psi S' \quad , \tag{B.15}$$

while

$$\Psi S \neq \Psi S' \quad . \tag{B.16}$$

Therefore, the expansion of Eq. (B.6) is not possible for arbitrary S. If S has a similar spectrum with fission spectrum χ, this expansion is supposed to be possible, but this possibility is not proved in this paper.

Acknowledgements

As long as we use the atomic energy in our lives, we can never forget the glory of Chicago Pile and the achievements of Dr Enrico Fermi and other scientists. Throughout our study in the master's course, we students have never forgotten the noble mind as little scientists, as Dr Pierre Curie taught us. I am thankful to professor Shiroya Seiji for giving us the best environment for study, and to associate professor Misawa Tsuyoshi and Dr Pyeon Cheolho for giving the shrewed advices and exact critics. Thanks to other students and staffs for the discussion and the daily support. May the atomic energy save the future.

References

1) Ewing, R. C., "High-level Nuclear Waste Immobilization with Ceramics," *Ceramics Int.*, **17**, 287-293 (1991).
2) Ewing, R. C., "Ceramic Matrices for Plutonium Disposition," *Prog. Nucl. Energy*, **49**, 635-643 (2007).
3) Salvatores, M., "Nuclear Fuel Cycle Strategies Including Partitioning and Transmutation," *Nucl. Eng. Des.*, **235**, 805-816 (2005).
4) Salvatores, M., "Fuel Cycle Strategies for the Sustainable Development of Nuclear Energy: The Role of Accelerator Driven Systems," *Nucl. Instrum. Method Phys. Res. A*, **562**, 578-584 (2006).
5) Herrera-Martínez, A., Kadi, Y., Parks, G., "Transmutation of Nuclear Waste in Accelerator-Driven Ssystems: Thermal Spectrum," *Ann. Nucl. Energy*, **34**, 550-563 (2007).
6) Herrera-Martínez, A., Kadi, Y., Parks, G., et al., "Transmutation of Nuclear Waste in Accelerator-Driven Ssystems: Thermal Spectrum," *Ann. Nucl. Energy*, **34**, 564-578 (2007).
7) Nishihara, K., Iwasaki, T., Udagawa, Y., "A New Static and Dynamic One-Point Equation and Analytic and Numerical Calculations for a Subcritical System", *J. Nucl. Sci. Technol.* **40**, 481-492 (2003).
8) Kobayashi, K., Nishihara, K., "Definition of Subcriticality Using the Importance Function for the Production of Fission Neutrons", *Nucl. Sci. Eng.* **136**, 272-281 (2000).
9) Misawa, T., Shiroya, S., "Measurement of Subcriticality by the Source Multiplication Method with a Detector Located at the Center of System," *Annu. Rep. Res. Reator Inst. Kyoto Univ.*, **26**, 125-128 (1993)
10) Misawa, T., "Subcriticality Measurement by Source Multiplication Method with Higher Mode Flux," JAERI-Conf 2002-004, 165-172 (2003).
11) Ogata, T., Master Thesis, Dept. of Fundamental Energy Sci., Facl. of Energy Sci. Kyoto Univ. (2004). (in Japanese)
12) Shibata, Y., Master Thesis, Dept. of Fundamental Energy Sci., Facl. of Energy Sci. Kyoto Univ. (2006). (in Japanese)
13) Kaneko, Y., "Integral-Versions of Some Kinetic Experiments for Determining Large Negative Reactivity of Reactor," *J. Nucl. Sci. Technol.*, **12**, 402-412 (1975).
14) Akino, F., Yasuda, H., Kaneko, Y., "Determination of Large Negative Reactivity by Integral Versions of Various Experiment Methods," *J. Nucl. Sci. Technol.*, **17**, 593-615 (1980).
15) Mizoo, N., "Theoretical and Experimental Studies on Measurement of Large Negative Reactivities," JAERI-M 7753 (1978). (in Japanese)
16) Tsuji, M., Suzuki, N., Shimazu, Y., "Subcriticality Measurement by Neutron Source Multiplication Method with a Fundamental Mode Extraction," *J. Nucl. Sci. Technol.*, **40**, 158-169 (2003).
17) Naing, W., Tsuji, M., Shimzau, Y., "Subcriticality Measurement of Pressurized Water Reactors by the Modified Neutron Source Multiplication Method," *J. Nucl. Sci. Technol.*, **40**, 983-988 (2003).
18) Okumura, K., Kugo, T., Kaneko, K., et al., "SRAC2006: A Comprehensive Neutronics Calculation Code System," JAEA-Data/Code, 2007-004 (2007).

19) Fowler, T. B., Vondy, D. R., Cunningham, G. W., "Nuclear Reactor Core Analysis Code: CITATION", ORNL-TM-2496 Revision 2 (1971).

20) Shibata, K., Kawano, T., Nakagawa, T., et al., "Japanese Evaluated Nuclear Data Library Version 3 Revision-3: JENDL-3.3," *J. Nucl. Sci. Technol.* **39**, 1125-1136 (2002).

21) Misawa, T., Yamamoto, A., Yamane, Y., "Application of Nodal Method to Lambda Mode Higher Harmonics Code," *J. Nucl. Sci. Technol.* **33**, 668-670 (1996).

22) Misawa, T., "Study on Nuclear Criticality Safety using Light Water Moderated and Reflected Cores Loaded with Highly Enriched Uranium Fuel," Doctor Thesis, Dept. of Nucl. Eng., Facl. of Eng., Kyoto Univ. (1989).

23) Shiroya, S., Kanda, K., Tsuchihashi, K., "Analyses of Reactor Physics Experiments in the Kyoto University Critical Assembly," *Nucl. Sci. Eng.*, **100**, 525-537 (1988).